Received: 24 November 2023 | Revised: 12 December 2023 | Accepted: 14 December 2023

DOI: 10.1111/mmi.15216

RESEARCH ARTICLE

WILEY

Diverse mechanisms control amino acid-dependent environmental alkalization by *Candida albicans*

Fitz Gerald S. Silao[1] | Valerie Diane Valeriano[2] | Erika Uddström[1] | Emilie Falconer[1] | Per O. Ljungdahl[1]

[1]Department of Molecular Biosciences, The Wenner-Gren Institute, Science for Life Laboratory (SciLifeLab), Stockholm University, Stockholm, Sweden

[2]Centre for Translational Microbiome Research (CTMR), Department of Microbiology, Tumor and Cell Biology, Karolinska Institute, Solna, Sweden

Correspondence
Fitz Gerald S. Silao, Department of Molecular Biosciences, The Wenner-Gren Institute, Science for Life Laboratory (SciLifeLab), Stockholm University, Stockholm, Sweden.
Email: fitzgerald.silao@su.se

Funding information
Vetenskapsrådet, Grant/Award Number: 2019-01547 and 2022-01190; HORIZON EUROPE Framework Programme, Grant/Award Number: ImResFun 606786

Abstract

Candida albicans has the capacity to neutralize acidic growth environments by releasing ammonia derived from the catabolism of amino acids. The molecular components underlying alkalization and its physiological significance remain poorly understood. Here, we present an integrative model with the cytosolic NAD^+-dependent glutamate dehydrogenase (Gdh2) as the principal ammonia-generating component. We show that alkalization is dependent on the SPS-sensor-regulated transcription factor *STP2* and the proline-responsive activator Put3. These factors function in parallel to derepress *GDH2* and the two proline catabolic enzymes *PUT1* and *PUT2*. Consistently, a double mutant lacking *STP2* and *PUT3* exhibits a severe alkalization defect that nearly phenocopies that of a *gdh2-/-* strain. Alkalization is dependent on mitochondrial activity and in wild-type cells occurs as long as the conditions permit respiratory growth. Strikingly, Gdh2 levels decrease and cells transiently extrude glutamate as the environment becomes more alkaline. Together, these processes constitute a rudimentary regulatory system that counters and limits the negative effects associated with ammonia generation. These findings align with Gdh2 being dispensable for virulence, and based on a whole human blood virulence assay, the same is true for *C. glabrata* and *C. auris*. Using a transwell co-culture system, we observed that the growth and proliferation of *Lactobacillus crispatus*, a common component of the acidic vaginal microenvironment and a potent antagonist of *C. albicans*, is unaffected by fungal-induced alkalization. Consequently, although *Candida* spp. can alkalinize their growth environments, other fungal-associated processes are more critical in promoting dysbiosis and virulent fungal growth.

KEYWORDS
alkalization, ammonia production, *Candida albicans*, *Candida auris*, *Candida glabrata*, glutamate dehydrogenase, human fungal pathogens, *Lactobacillus crispatus*, mitochondria, oxygen, proline catabolism, virulence

1 | INTRODUCTION

Candida albicans is the primary cause of human mycoses presenting a spectrum of pathologies ranging from superficial lesions to life-threatening invasive infections. Recently, the World Health Organization (WHO) listed *C. albicans* under its "critical priority" group of fungal pathogens alongside the newly characterized multidrug-resistant *Candida auris* (Fisher & Denning, 2023; WHO, 2022). Despite its ill repute, *C. albicans* is normally a harmless commensal, thriving as a benign member of human microbiota in healthy individuals. Amino acids are among the most abundant nutrients in human hosts capable of supporting fungal growth. However, the utilization of amino acids must be controlled due to the risk of accumulating ammonia (NH_3), a weak base that becomes toxic when in excess (Vylkova, 2017). The release of ammonia (NH_3) into the extracellular space alkalinizes the growth environment as it converts to ammonium (NH_4^+) (Vylkova et al., 2011). The interest in studying this process in *C. albicans* is linked to findings that alkaline pH induces filamentous growth in vitro; morphological switching is a known virulence characteristic. Extracellular alkalization via ammonia release is not exclusive to *C. albicans*, other members of the pathogenic *Candida* species complex are also capable of alkalinizing their growth environments, albeit to varying degrees and dependent on the medium used (Kasper et al., 2014; Vylkova et al., 2011). For example, *Candida glabrata*, a WHO "high priority" fungal pathogen, can only alkalinize a medium containing amino acids as a sole source of carbon and nitrogen (Kasper et al., 2014); the addition of other carbon sources like glycerol abrogates alkalization (Vylkova et al., 2011).

We recently reported that the NAD^+-dependent glutamate dehydrogenase (Gdh2; EC:1.4.1.2), which catalyzes the deamination of glutamate to α-ketoglutarate (Han et al., 2019; Silao et al., 2019, 2020), is the key enzyme responsible for ammonia generation during growth on amino acids (Silao et al., 2020). Deletion of *GDH2* completely abrogated both the ability of strains to generate ammonia and alkalinize amino acid-based media, even during extended periods of incubation (Silao et al., 2020). The alkalization defect of a *gdh2* mutant surpassed the prominent alkalization deficiency observed in a strain lacking *STP2* (Silao et al., 2020), which has been extensively referenced as an alkalization-deficient strain (Danhof et al., 2016; Hollomon et al., 2022; Miramon et al., 2020; Miramon & Lorenz, 2016; Todd et al., 2019; Vylkova et al., 2011; Vylkova & Lorenz, 2014). *STP2* encodes a transcription factor required to derepress the expression of several amino acid permease genes and a subset of oligopeptide transporters (Martinez & Ljungdahl, 2005; Miramon & Lorenz, 2016). Stp2 is produced as a latent precursor that is proteolytically activated by the concerted action of the SPS (Ssy1-Ptr3-Ssy5) sensor in response to the presence of extracellular amino acids. The processed form of Stp2, lacking an N-terminal cytoplasmic retention domain, efficiently translocates to the nucleus where it binds to promoters of target genes (Martinez & Ljungdahl, 2005; Miramon & Lorenz, 2016; Silao et al., 2019). In addition to the alkalization deficiency, *stp2* mutants were found to exhibit reduced virulence in mouse bone marrow-derived macrophages and/or in murine systemic infection models (Amorim-Vaz et al., 2015; Danhof & Lorenz, 2015; Vesely et al., 2017; Vylkova & Lorenz, 2014). These findings suggested a link between alkalization and virulence. Specifically regarding macrophages, ammonia extrusion was postulated to provide *C. albicans* (Danhof & Lorenz, 2015; Vylkova & Lorenz, 2014) and *C. glabrata* (Kasper et al., 2014) the means to increase the pH within the phagosomal compartment, enhancing their survival and their ability to evade macrophages. This notion is inconsistent with recent data. The inactivation of *GDH2* does not affect *C. albicans* virulence in a murine systemic infection model, nor prevents morphological switching or survival of cells phagocytized by macrophages (Silao et al., 2020). Furthermore, we and others have shown using independent imaging-based methods (i.e., pHrodo Silao et al., 2020 and ratiometric Westman et al., 2018) that phagosomes engulfing wildtype *C. albicans* cells remain acidic and that the observed phagosomal alkalization, if any, is a result of membrane distention as hyphae extend (Westman et al., 2018). Thus, Stp2-regulated gene expression must be linked to other processes affecting virulence.

Mitochondrial function is key to effect alkalization, which occurs only when cells are grown under respiratory conditions, i.e., medium with low (<0.2%) glucose or alternative carbon sources, such as glycerol and/or lactate (Silao et al., 2020; Vylkova et al., 2011). The Proline UTilization (PUT) pathway, a major pathway for the generation of glutamate, is comprised of Put1 (proline dehydrogenase; EC 1.5.5.2) and Put2 (Δ1-pyrroline-5-carboxylate (P5C) dehydrogenase; EC 1.2.1.88) that are localized exclusively in the mitochondria (Silao et al., 2020, 2023). Under respiratory conditions, strains lacking *PUT1* and *PUT2* exhibit significantly reduced capacities for alkalinizing the growth media, indicating the presence of other pathways to generate glutamate (Silao et al., 2019, 2020). Interestingly, in contrast to mammalian cells, where the NAD^+-dependent glutamate dehydrogenase (GDH) is localized to the mitochondria and the α-ketoglutarate formed from glutamate feeds directly into the TCA cycle, Gdh2 in *C. albicans* is a cytoplasmic enzyme (Silao et al., 2020, 2023). This difference raises the question as to how *C. albicans* cells coordinate reactions occurring in spatially exclusive sites to properly control the effects of environmental alkalization.

Here, we present an integrative model that accounts for how *C. albicans* generates ammonia and initiates the neutralization of acidic environments. Our work was based on testing the hypothesis that Gdh2 is the critical component, which enabled us to evaluate the contributions and connections of other known factors linked to amino acid uptake and mitochondrial function. Consistent with our finding in *C. albicans*, we show that although *GDH2* is essential for amino acid dependent-alkalization in other pathogenic *Candida* species, including *C. glabrata* and *C. auris*, it remains dispensable for virulence as assessed by survival in whole blood culture. Furthermore, by examining the proliferation of *Lactobacillus crispatus*, a potent antagonist of *C. albicans* that normally thrives in the acidic vaginal microenvironment, we found that environmental alkalization does not directly limit the growth of this competing microorganism.

2 | RESULTS

2.1 | Gdh2 level is sensitive to extracellular pH

Gdh2 levels decrease as the pH of the growth medium increases toward neutrality (Silao et al., 2020). Previously, we have shown that the rate of alkalization is highly dependent on the starting cell density; dense cultures ($OD_{600} \geq 2$) alkalinize the medium faster than diluted cultures (Silao et al., 2020). Based on the more rapid and stringent output, we have used high-density cultures to assess the alkalization potential of *C. albicans* strains. To directly examine the effect of pH on Gdh2 stability, strain CFG433 was pre-grown in YPD to fully repress Gdh2 expression and cells were subsequently shifted to a synthetic medium containing casamino acids (CAA) as the sole carbon/nitrogen/energy source (YNB+CAA; pH=4, unbuffered) for 2h to induce the expression of Gdh2. Following induction, the cultures were added with buffers at defined pHs ranging from 4 to 8, spiked with cycloheximide (CHX) to arrest translation, and then the levels of Gdh2 were monitored after 1h (Figure 1a). Relative to T = 0h immediately after adding CHX, there was no significant change in Gdh2 levels at pH=4, indicating that Gdh2 is relatively stable at acidic pH (Figure 1b). Interestingly, a significant drop in the levels of Gdh2 was observed at a pH of 5. Similarly, the levels of Gdh2 in the unbuffered control culture, where the pH increased to ~5 (see wells in Figure 1a), significantly decreased. The strain CFG433 also co-expresses Put1-RFP and Put2-HA, which enabled us to simultaneously assess the levels of three proteins in a single blot. In contrast to Gdh2, both Put1 and Put2 were stable under all the pH conditions tested (Figure 1b), suggesting that the capacity to generate glutamate in the mitochondria from proline remained unchanged. Consequently, we posited that the reduced levels of cytosolic Gdh2 may reflect an active control mechanism that engages to limit the production of ammonia as the external pH increases. To directly test this notion, we examined the capacity of cells, grown at different starting pHs to alkalinize the culture media. Cells were pre-grown in YNB+CAA medium (pH=4) for 2h prior to shifting them to YNB+CAA with an initial pH (pH_i) of 4 or 6. The pH of the media were assessed after 3h (pH_{3h}) (Figure 1c). Gdh2 levels were clearly lower in cells shifted to pH6; however, detectable levels of Gdh2 remained (Figure 1b). Consistent with this, the change in pH ($\Delta pH = pH_{3h} - pH_i$) was significantly lower in cells shifted to pH_i of 6 than 4, $\Delta pH = 1.3$ versus $\Delta pH = 2.8$, respectively (Figure 1c). This is despite the fact that the resulting pH (pH_{3h}) of the growth medium was significantly higher at pH_i of 6 ($pH_{3h} = 7.3$) compared to that of cells shifted to pHi of 4 ($pH_{3h} = 6.8$; Figure 1c). These results are consistent with the existence of a pH-sensitive regulatory mechanism that constrains the alkalization potential of *C. albicans*.

2.2 | High glucose and mitochondrial activity regulate glutamate availability for Gdh2

Previous studies have shown that high (2%) levels of glucose in CAA-based media inhibit extracellular alkalization (Vylkova et al., 2011). Consistently, we have found that cells grown in the presence of high glucose express significantly lower levels of Gdh2 (Figure 2a). Consequently, cells grown in the presence of high glucose are expected to have a limited capacity to produce ammonia. We have previously shown that the components of the proline utilization (PUT) pathway, Put1 and Put2, generate glutamate in the mitochondria and are also repressed in cells grown with high glucose (Silao et al., 2019, 2020). Immunoblot analysis of Gdh2 and Put2 confirms this (Figure 2a), and consistently, the level of intracellular glutamate was significantly lower in cells grown in a medium containing 2% glucose (Figure 2b).

In addition to limiting the levels and deamination of glutamate, high glucose pleiotropically represses mitochondrial activity, which can affect the movement of metabolites between the cytosol and the mitochondria (Silao & Ljungdahl, 2021). Consistently, and supporting the notion that mitochondrial activity is essential to alkalization, we have shown that alkalization is blocked by the potent mitochondrial complex III inhibitor antimycin A (AntA) (Silao et al., 2020). Based on the assumption that the bulk of cytoplasmic glutamate originates from the mitochondria, we considered the possibility that acute inhibition of mitochondrial function would reduce the cytoplasmic glutamate levels, presumably due to an impaired capacity to transport glutamate out of the mitochondria. To test this, we analyzed the level of glutamate in the cytosol of the reporter strain (CFG441) grown in YNB+CASG (i.e., YNB+CAA medium supplemented with 38mM ammonium sulfate and 1% glycerol) 30min after inhibition by AntA (1μg/mL) (Figure 2c, top panel). Having found that alkalization reduces Gdh2 levels (Figure 1b), we deliberately limited the analysis of expressed enzyme levels to 30min after the addition of AntA. The cytosol fraction was extracted using the procedure reported by Ohsumi et al. (1988) using dilute $CuCl_2$ (0.2mM) to gently

FIGURE 1 The level of Gdh2 is sensitive to extracellular pH. (a) Scheme for the alkalization experiment. Gdh2 was induced for 2h in YNB+CAA with bromocresol purple (BCP) as pH indicator and then spiked with concentrated buffer to 50mM final concentration and cycloheximide (CHX) to arrest translation. Cultures were incubated for another 1h followed by whole cell lysis and immunoblotting. (Right panel) Aliquots of spiked cultures after 1h were placed in microplate wells to show the change in color corresponding to the indicated pH. (b) Immunoblot and quantification of Gdh2-GFP, Put1-RFP, and Put2-HA levels in cells grown at different culture pH. The signals from the target proteins were first normalized to α-tubulin and then compared relative to T=0h (set to 1). Data presented are from 4 biological replicates (mean with 95% CI; analyzed by one way ANOVA followed by Dunnett's posthoc test, $^{****}p < 0.0001$). (c) Alkalization rate is slower at elevated pH. Gdh2 was first induced to maximal expression in YNB+CAA and then shifted to YNB+CAA with initial pH (pHi) of 4 or 6 followed by incubation for 3h. Resulting pH values were deducted from pHi to obtain ΔpH. Box and Whiskers plot with minimum and maximum values derived from 6 biological replicates analyzed by unpaired student *t*-test, $^{**}p < 0.01$, $^{****}p < 0.0001$).

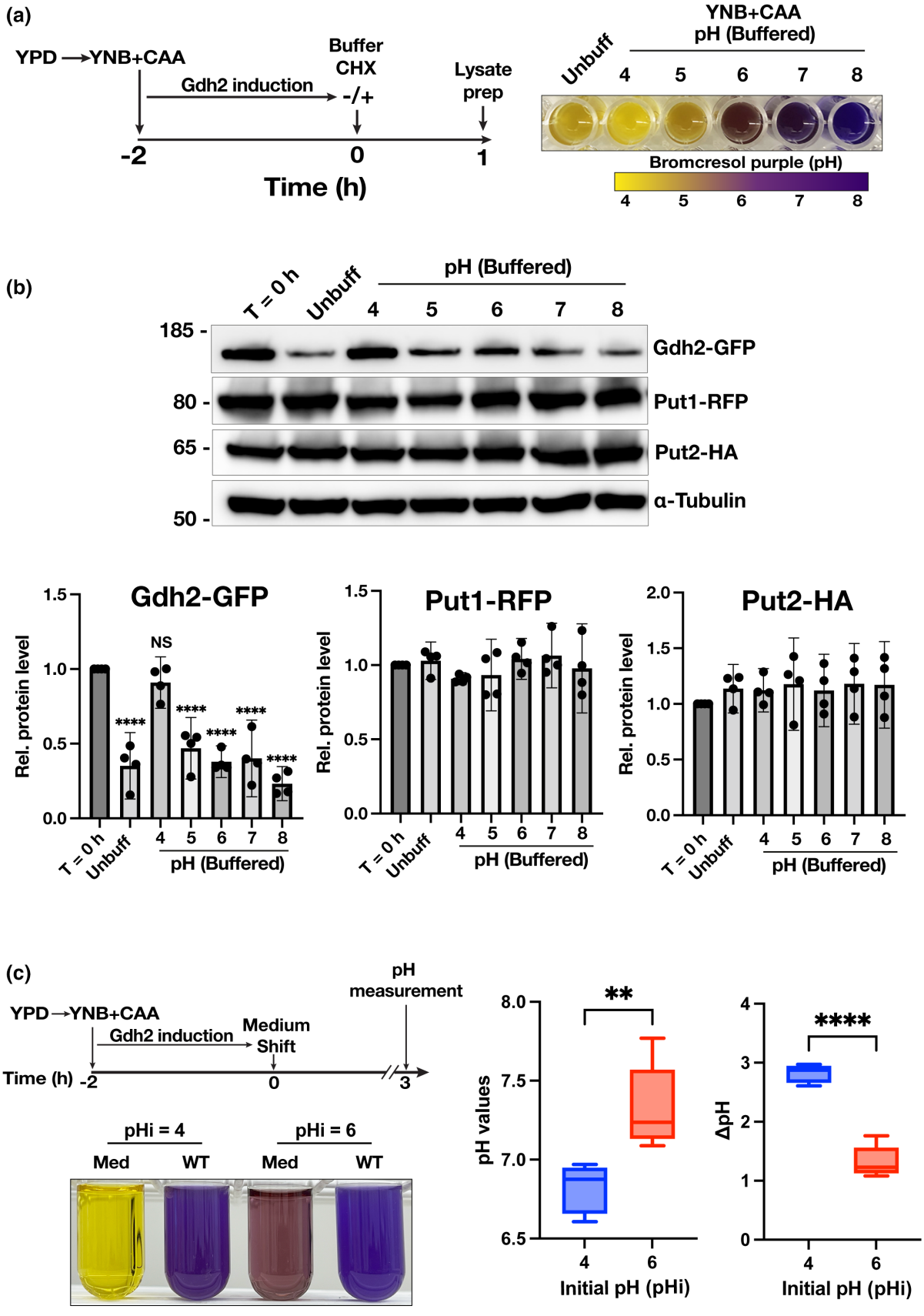

permeabilize the plasma membrane. We observed a significant ~3-fold reduction in the level of cytosolic glutamate following treatment by AntA (Figure 2c). As expected, alkalization was arrested by AntA as inferred by the lack of color change of the pH indicator (Figure 2c). Consistent with glutamate being limiting, the level of α-ketoglutarate was also significantly reduced (Figure 2c). Under these conditions, the levels of Gdh2, Put1, and Put2 remained unchanged (Figure 2d).

To further test the role of mitochondria in alkalization, we examined a strain lacking *NUO1*, which encodes a subunit of mitochondrial NADH:ubiquinone oxidoreductase (complex I). The *nuo1*Δ/Δ manifests the classical mitochondrial-deficient phenotypes, including reduced respiration (oxygen consumption), low mitochondrial membrane potential, and extremely poor growth on non-fermentable carbon sources (Huang et al., 2017; She et al., 2015). A dense culture of wildtype cells in YNB + CASG (OD_{600} of 5) becomes alkaline within 3 h. In contrast, similar cultures of a *nuo1*Δ/Δ strain fail to alkalinize the medium even after 8 h, although the cultures eventually became alkaline after 24 h incubation (Figure 2e). Finally, a simple classical experiment, based on incubating dense cultures statically at room temperature, revealed that alkalization occurs only within the upper layer exposed to the atmosphere, clearly demonstrating that alkalization is linked to respiratory growth (Figure 2f). Together, these results support the scheme shown in Figure 2g in which mitochondria actively contribute to the activity of Gdh2 by supplying the cytoplasmic localized Gdh2 with glutamate produced via proline catabolism (PUT) and/or mitochondrial-localized aminotransferases (AT; Silao & Ljungdahl, 2021).

2.3 | Glutamate excretion enables cells to transiently dispose of excess nitrogen

Based on our findings that the levels of Gdh2, but not that of PUT enzymes, decrease as the extracellular pH rises above 5 (Figure 1b), we posited that the size of the intracellular glutamate pool would increase in parallel with increasing pH. We considered the possibility that excess glutamate could be metabolized to support the biosynthesis of other amino acids, e.g., glutamine (Silao & Ljungdahl, 2021), or alternatively, be excreted to the extracellular environment. Either of these processes could individually or together decrease the intracellular glutamate pools and reduce the possibility to generate ammonia. Amino acid excretion has been reported to occur in *S. cerevisiae* (Velasco et al., 2004); however, this has not been adequately addressed in *C. albicans*. Amino acid excretion has only been observed in studies analyzing spent growth medium from *C. albicans* biofilm cultures (Bottcher et al., 2022).

We measured the level of extracellular glutamate 3 and 5 h after growth in a glutamate-devoid minimal medium supplemented with amino acids that can be metabolized to glutamate (Silao & Ljungdahl, 2021); this YNB + PALAAG medium contains 0.5 g/L of Proline, Arginine, Leucine, Alanine, and Aspartate, and 1% Glycerol as primary carbon source. Extensive washing (4×) of the pre-cultured YPD grown cells was crucial to remove contaminating amino acids, including glutamate, prior to shifting cells to YNB + PALAAG. We chose 3 h as the earliest time point as this correlates with the dramatic reduction in Gdh2 levels in cells growing in the unbuffered YNB + CAA medium (Figure 1). Consistent with expectations, we detected substantial amounts of glutamate in the spent medium from wildtype cultures (Figure 3). Strikingly, 2 h later, i.e., 5 h post shift, we observed a ~20-fold reduction of extracellular glutamate, suggesting that glutamate is transported back into cells. The spent medium from cultures of the *gdh2*−/− mutant also contained glutamate, however, at significantly lower levels than wildtype ($p < 0.0001$; Figure 3). In clear contrast to wildtype, the extracellular glutamate levels increased in the *gdh2*−/− strain, indicating continued excretion. Together, these results indicate that glutamate excretion provides *C. albicans* cells the alternative to dispose of excess nitrogen without the negative effects of ammonia-dependent alkalization.

2.4 | Stp2 and Put3 are key regulators of Gdh2, Put1, and Put2 expression

Next, we pursued the mechanisms underlying the induced expression of Gdh2 in strains growing in CAA-based medium. Interestingly, Gdh2 induction occurs independent of its substrate glutamate, but rather exhibits dependency on the proline-sensitive transcription factor Put3 (Silao et al., 2023) and SPS sensor-regulated Stp2 (Vylkova & Lorenz, 2014). Based on transcriptional profiling, these factors act in positive manner (Miramon et al., 2020; Tebung et al., 2017). Also, additional factors must contribute, since arginine-dependent induction of Gdh2 occurs in strains lacking *PUT3* (Silao et al., 2023). To critically assess the action of these factors, we inactivated *STP2* or/and *PUT3* in strain CFG441 (Figure S1A) and tested the capacity of the mutant strains to alkalinize YNB + CASG medium (Figure 4a, upper panel). The application of CRISPR/Cas9 enabled the simultaneous inactivation of all three *STP2* alleles (Figure S1A; Martinez & Ljungdahl, 2005); from here onward, *stp2*−/−/− is designated as *stp2-/-* or *stp2*. As in previous reports, the *stp2* strain showed a clear defect in alkalization even at high density (OD ≈ 5; Figure 4a, upper panel); however, media alkalization was observed upon prolonged incubation (24 h). The *put3* strain showed a modest but significant delay in alkalization (Figure 4a, lower panel). Strikingly, the *stp2 put3* double mutant showed a severe alkalization defect that clearly surpassed that of *stp2* mutant and that almost phenocopied the clear alkalization defective phenotype of the *gdh2* mutant (Figure 4a). Relative to YNB + CASG, the *stp2* or *stp2 put3* mutants showed an even more prominent defect in YNB + CAA after 24 h (Figure S1B), likely due to the tight dependency of amino acid uptake on Stp2. We inactivated *PUT3* in the previously reported *stp2*Δ/Δ strain (Vylkova & Lorenz, 2014) and obtained identical results.

These findings prompted us to directly examine Gdh2 levels. Importantly, since extracellular alkalization negatively affects Gdh2 levels (Figure 1b), we limited the analysis to cultures grown only for 2 h post-YPD shift. The results clearly show that Stp2 and Put3 co-regulate Gdh2 expression, with Stp2 having a more dominant role

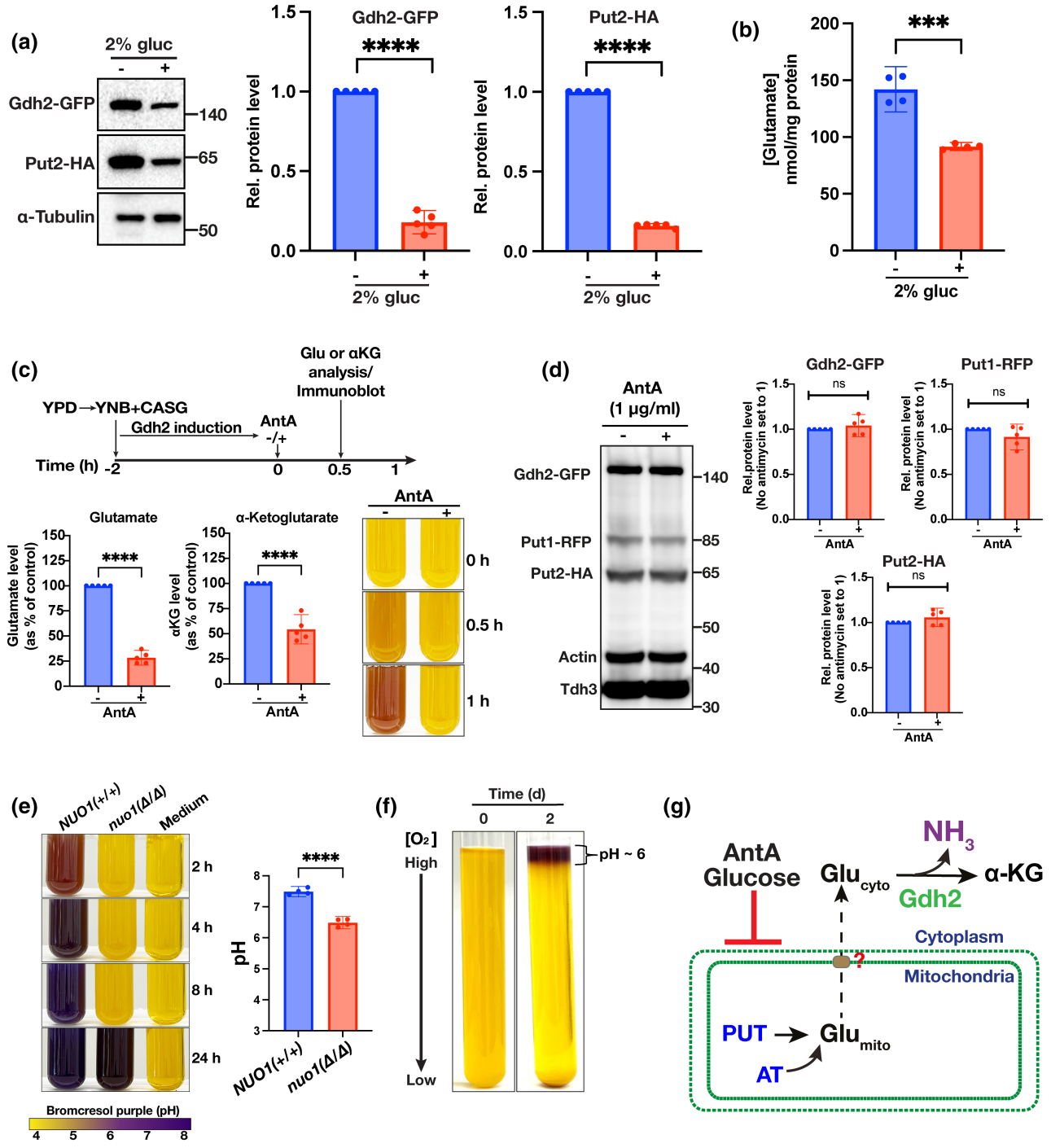

FIGURE 2 High glucose and mitochondrial activity regulate glutamate availability for Gdh2. (a) Glucose availability inversely affects cytoplasmic glutamate levels. Immunoblot analysis of Gdh2-GFP and Put2-HA levels in lysates prepared from cells (CFG404) grown in YNB+CAA without or with 2% glucose. (b) Intracellular glutamate levels in lysates prepared from (a). Data shown were obtained from 4 to 5 biological replicates (mean with 95% CI; ***$p<0.0001$ by student *t*-test). (c) Mitochondrial function is required to maintain cytoplasmic glutamate levels. Cells were grown for 2 h in YNB+CAA medium to induce Gdh2 expression and then spiked with Antimycin A (AntA) or vehicle control (ethanol, −). Tubes were photographed at the indicated timepoints (Right) or sampled after 30 min to determine the levels of cytosolic glutamate and α-ketoglutarate (Left); results are presented as percentage (%) of vehicle control derived from 5 biological replicates (mean with 95% CI; ****$p<0.0001$ by student *t*-test). (d) Immunoblot analysis of cells grown and sampled as in (c). Enzymes levels are not altered after exposing the cells to AntA. Enzymes were simultaneously detected in the same lysate and quantified using Tdh3 as loading control. Data is presented as mean with 95% CI ($n=5$). (e) Strain with mitochondrial dysfunction exhibits striking alkalization defect. (Left) Wildtype *NUO1*+/+ (SN250) and *nuo1*Δ/Δ (CB342) strains were grown in YNB+CASG at OD ≈ 5 and photographed at the indicated timepoints. (Right) pH values of cultures after 24 h (mean with 95% CI; ****$p<0.0001$ by student *t*-test). (f) CFG441 cells were inoculated into 20 mL of YNB+CAA at OD ≈ 5 and then kept upright at room temperature for 2 days. Only the top layer with the highest oxygen concentration resulted to alkalization. (g) Schematic diagram of AntA or high glucose inhibits alkalization. AntA or high glucose inhibits mitochondrial function and prevent the export of Glu_{mito} generated by either proline catabolism (PUT) or aminotransferases (AT) to the cytosol.

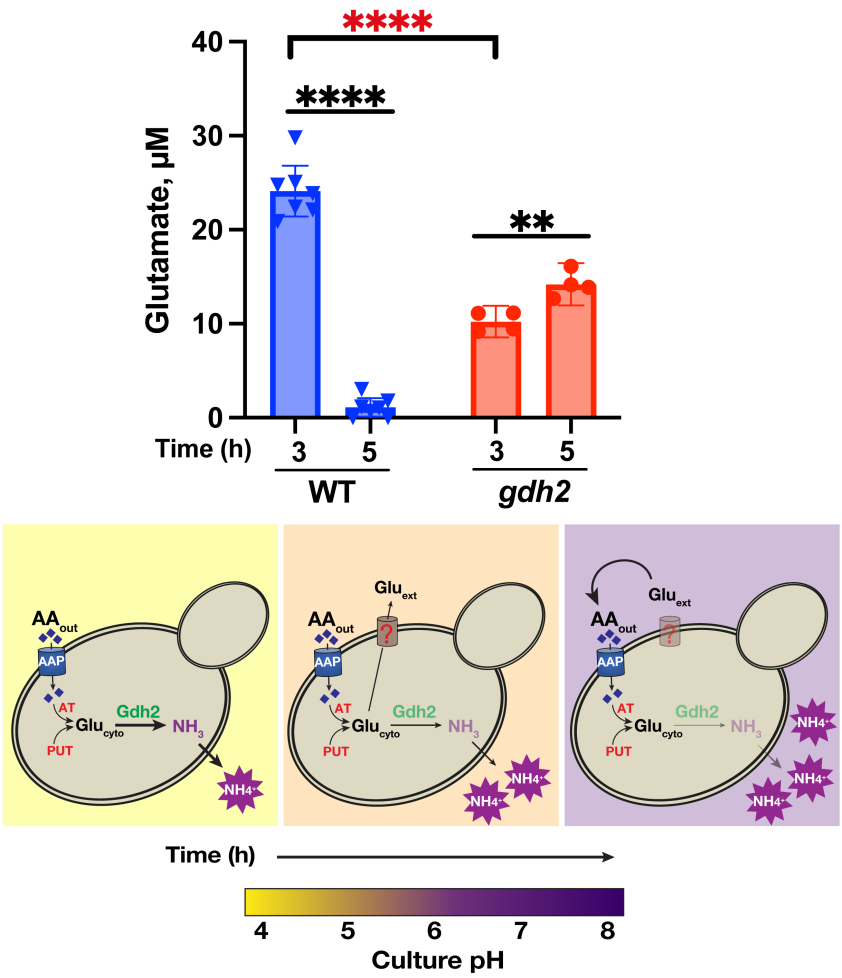

FIGURE 3 Glutamate extrusion in *Candida albicans* as a mechanism to regulate intracellular glutamate pool. (Upper panel) Glutamate levels in YNB + PALAAG medium grown with WT (SC5314) and *gdh2* (CFG279) cells taken at the indicated timepoints. Data shown were obtained from seven (WT) and four (*gdh2*) biological replicates (mean with 95% CI; $^{****}p < 0.0001$ and $^{**}p < 0.01$ by student *t*-test; red asterisks denote comparison between WT and *gdh2* at 3 h timepoint). (Lower panel) Schematic diagram of glutamate extrusion in *C. albicans* as a function of time. Cytosolic glutamate (Glu_{cyto}) generated from aminotransferases (AT) reactions or proline catabolism (PUT) are converted by Gdh2 to ammonia (NH_3), which neutralizes the extracellular space. As the pH increases, Gdh2 level decreases which provide a surplus of Glu_{cyto} that are then extruded to the medium and then reassimilated.

in its regulation compared to Put3 (Figure 4b). Surprisingly, Stp2 also regulates Put1 and Put2 as indicated by their reduced levels in the *stp2* strain. Interestingly, Put1 expression exhibited a tighter requirement for Stp2, whereas Put2 expression was more Put3-dependent. Put3 levels were not altered in a *stp2* mutant (Figure 4c). In all cases, the difference between *stp2* and *stp2 put3* were always significant (Figure 4b, red asterisks), suggesting that Stp2 and Put3 operate independently and in parallel to regulate the expression of *GDH2*, *PUT1*, and *PUT2*.

The PathoYeastract (Teixeira et al., 2023) and/or YeTFaSCo (de Boer & Hughes, 2012) databases were used to analyze the 1000 bp region preceding the *GDH2* ORF. A putative Put3-binding motif [CGG(Nx)CCG] (Swaminathan et al., 1997) positioned at −866 from the ORF was found (Figure 4d), as were two Stp2 binding motifs at positions −137 and/or −874 [CGGCTC (de Boer et al., 2000) and/or GYGCCGYR (Yang & Wu, 2012) 1 bp substitution allowed]. Interestingly, Stp2 is not in the list of transcription factors associated with either *PUT1* or *PUT2* regulation, although we found positions −153/−668 (*PUT1*) and −197 (*PUT2*) resembling Stp2 binding motifs (de Boer et al., 2000; Yang & Wu, 2012). Further analyses of these promoter regions identified the presence of bindings motifs for Mig1 and Mig2, which are partially redundant orthologs mediating glucose repression in *C. albicans* (Lagree et al., 2020); [*GDH2* (−376), *PUT1* (−165, −651, −722, −937), and *PUT2* (−94, −163)]. The putative involvement of Mig1 and Mig2 is consistent with our findings that Gdh2, Put1 and Put2 levels are lower in high glucose grown cells (Silao et al., 2019, 2020). In summary, the results strongly suggest that the prominent alkalization defect observed in the *stp2* mutant is primarily the consequence of reduced levels of Gdh2, Put1, and Put2.

2.5 | The role of Gdh2 is conserved in other pathogenic *Candida* species

The capacity to neutralize the environment in the presence of amino acids was reported previously in other members of the pathogenic *Candida* species complex (Vylkova et al., 2011), including the multidrug resistant *C. auris* (Smith et al., 2022) and *C. glabrata* (Kasper et al., 2014). To test whether Gdh2-dependent alkalization is conserved in these species, we created *GDH2* deletions in *C. auris* and *C. glabrata* by homology-directed recombination using an HA-tagging cassette (pFA6a-3HA-SAT-flipper) derived from the original SAT1-flipper cassette (Reuss et al., 2004). We created reconstituted strains following the procedure described previously in *C. albicans* (Silao et al., 2020; Figure 5a). We compared the alkalization capacity of each strain grown in dense cultures (OD ≈ 5). Interestingly and consistent with a previous report (Vylkova et al., 2011), *C. glabrata* does

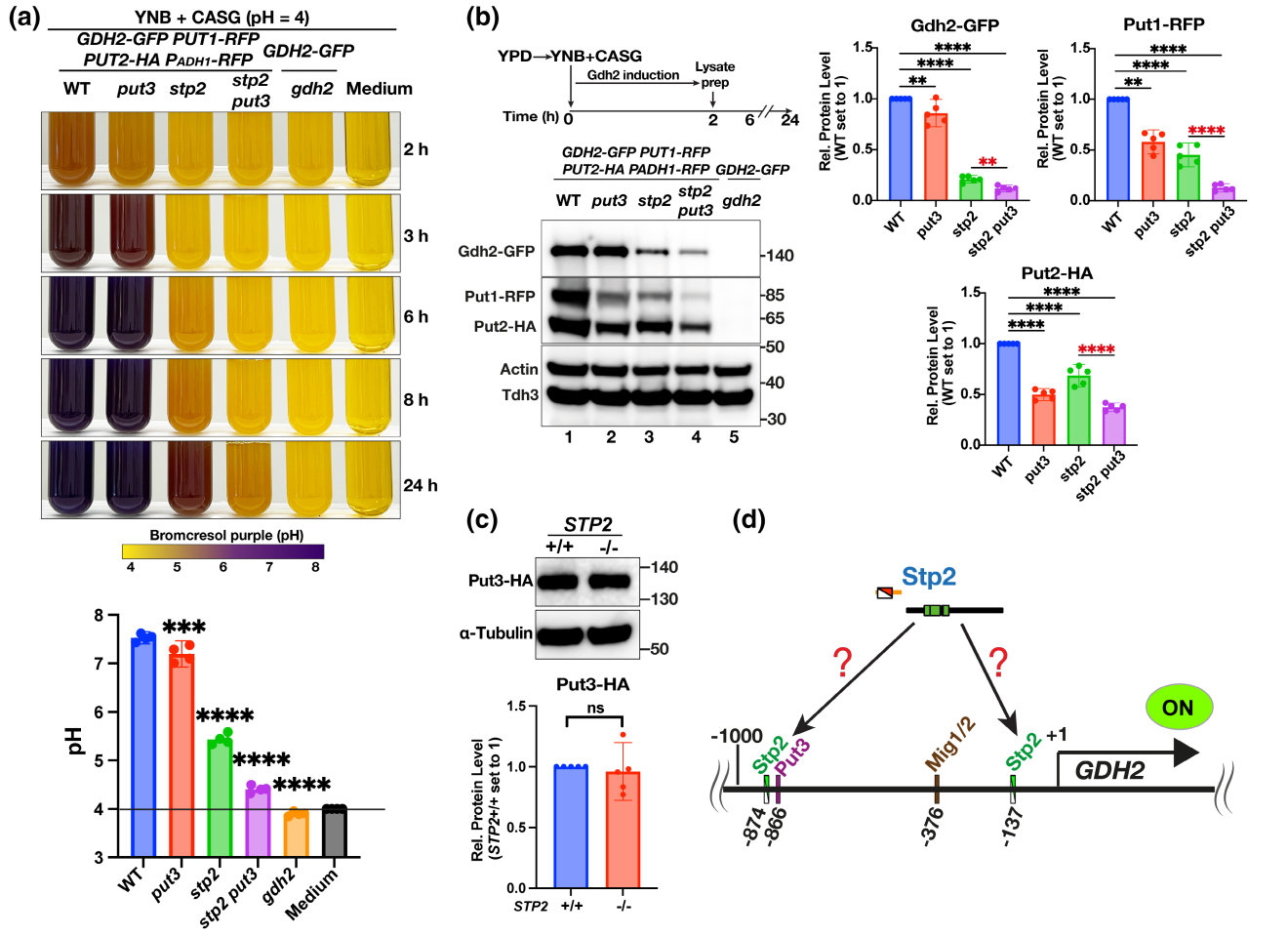

FIGURE 4 Gdh2 expression is co-regulated by Stp2 and Put3. (a) Cells of the following genotypes were grown in YNB + CASG at OD ≈ 5 and then photographed at the indicated timepoints (Top) and corresponding pH after 24 h (Bottom). Strains used are as follows: WT (CFG441), *put3* (CFG443), *stp2* (CFG665), *stp2 put3* (CFG671), and *gdh2* (CFG412). (b) Immunoblot analysis of Gdh2-GFP, Put1-RFP, and Put2-HA in the same strains as in (a) grown for 2 h in YNB + CASG at starting OD ≈ 2. Data are presented as Relative (Rel.) protein level (mean with 95% CI, $n = 5$; $^{****}p < 0.0001$, $^{**}p < 0.01$ by one way ANOVA with Dunnett's post hoc test); Signals were first normalized to loading control (Tdh3) and then transformed the values relative to WT set to 1. Red asterisks indicate localized comparison by student *t*-test. (c) Put3 expression is independent of Stp2. Strains CFG233 (*PUT3-HA*) and CFG676 (*PUT3-HA stp2–/–*) were grown to log phase in SGL medium and then processed for immunoblotting to detect the levels of Put3-HA. Representative immunoblot (left) and quantification (right) derived from 5 biological replicates (mean with 95% CI). (d) Proposed model of *GDH2* regulation by Stp2. Stp2 directly regulates *GDH2* by binding directly to the upstream activating sequence (UAS) in its promoter or indirectly through regulation of an intermediate TF that directly activates *GDH2*. The presence of Stp2, Put3 and Mig1/2 binding motifs in the promoter of *GDH2* were predicted using PathoYeastract (Teixeira et al., 2023) and/or YeTFaSCo (de Boer & Hughes, 2012) databases.

not readily alkalinize the extracellular medium (YNB + CASG) even after 72 h of prolonged growth (Figure 5b). However, when we grew the wildtype or reconstituted strain (*gdh2*Δ::*GDH2*) in YNB + CAA, where amino acids are used as sole carbon/nitrogen/energy source, alkalization was evident after ~5–6 h of growth being more pronounced after 8 h (Figure 5b). As expected, the Cg*gdh2* strain is completely unable to alkalinize the medium even after prolonged incubation (32 h). Unlike *C. glabrata*, the wildtype *C. auris* strain robustly neutralized the YNB + CASG medium, and as expected, the Cau*gdh2* strain did not, even after extended incubation beyond 24 h (Figure 5c). The results suggest that consistent with the role of Gdh2 in *C. albicans* (CaGdh2), the Gdh2 orthologues in *C. auris* (CauGdh2) and *C. glabrata* (CgGdh2) are also essential for amino acid-dependent alkalization. Analysis of the N-termini of CauGdh2 (B9j08_004192p) or CgGdh2 (CAGL0G05698g) by MitoFates (Fukasawa et al., 2015) revealed no mitochondrial pre-sequence (probability ~0.00) suggesting that these enzymes, as in *C. albicans*, localize to the cytoplasm.

Gdh2 is dispensable for the virulence of *C. albicans* (Silao et al., 2020). To assess the role of Gdh2 in virulence of *C. auris* and *C. glabrata*, we first assayed the survival of the wildtype and *gdh2* strains using a human whole blood infection model (Kammer et al., 2020). Consistent with our findings in *C. albicans*, Gdh2 is dispensable for virulence of these two *Candida* species as there was no significant difference in the survival of *gdh2* mutant in either species relative to their respective wildtypes (Figure 5d). We also tested the importance of *GDH2* in the capacity of *C. glabrata* to specifically

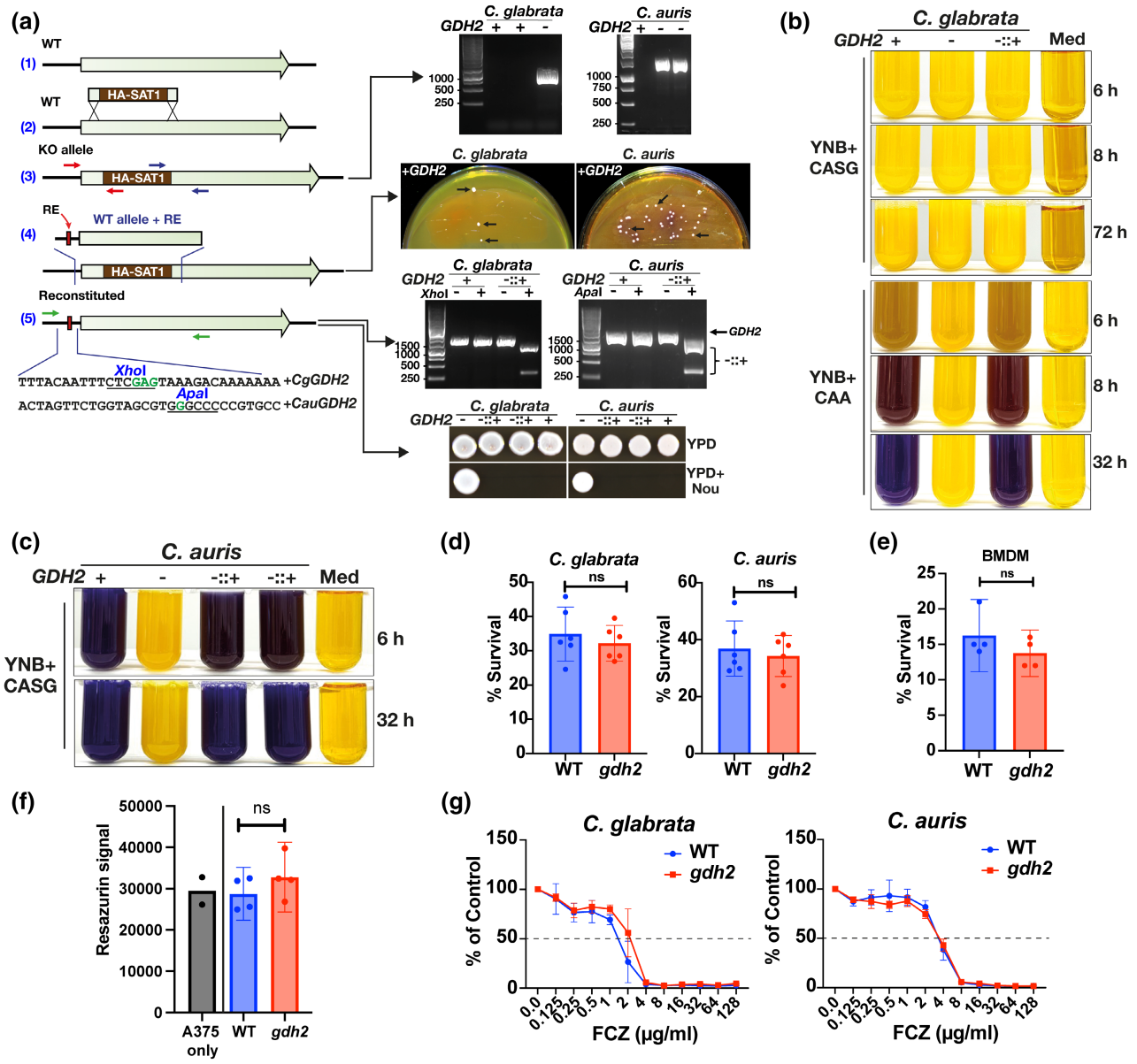

FIGURE 5 Gdh2 function is conserved in other *Candida* species. (a) Genetic construction of *gdh2* and reconstituted *C. glabrata* and *C. auris* strains. A region of the wildtype (WT) gene (1) was deleted by homology-directed recombination using a cassette amplified from a plasmid derivative of the SAT1-flipper cassette (2) and correct integration was verified by PCR using one of the primer pairs indicated in the scheme (3). The corresponding gels on the right used the primer pairs in blue. For reconstitution, the deleted region was replaced by WT allele bearing restriction sites (RE) (4) that were inserted in the primers (5, green font). Transformation was made on YNB + CAA plate and colonies pointed with arrows (4) were analyzed by PCR and restriction digest using either *Xho*I (*C. glabrata*) or *Apa*I (*C. auris*) (5). The reconstituted strains lost the nourseothricin resistance marker as indicated by the lack of growth on YPD with 200 μg/mL nourseothricin (+Nou). (b, c) Wildtype (+), *gdh2* (−), and reconstituted (−::+) strains of *C. glabrata* (b) and *C. auris* (c) were grown in the indicated alkalization medium at OD ≈ 5 and photographed at the indicated timepoints. (d) *GDH2* is dispensable for survival of *C. glabrata* and *C. auris* in a human blood infection model. Cells (~10^5 CFU) were added into a blood aliquot and survival was assessed 1 h after by plating. Data shown were obtained from six independent donors (mean with 95% CI; not significant by student *t*-test). (e) *GDH2* is not required for immediate survival of *C. glabrata* following interaction with macrophages. Survivals of antibody-opsonized fungal cells were calculated by comparing the recovered CFU after 2 h of incubation with macrophages to the initial CFU. Data ($n = 4$) were analyzed by student *t*-test (ns = not significant). (f) *GDH2* is not required for the cytotoxic effects of *C. auris*. Cytotoxicity was assessed using resazurin reduction assay on a confluent monolayer of A375 cells infected with wildtype and *gdh2* strains for 24 h. Data ($n = 4$) between wildtype and *gdh2* strains were analyzed by student *t*-test. (g) *GDH2* is not required for fluconazole (FCZ) susceptibility of *C. glabrata* and *C. auris*. Growth (as OD) of the indicated strains in increasing concentrations of fluconazole was measured at 24 h. Growth inhibition of 50% (MIC) relative to untreated control is shown as a dotted horizontal line. Each data point represents mean ± SD ($n = 3$–4). Strains used are as follows: *C. glabrata* – wildtype (+, ATCC 2001), *gdh2* (−, CFG670), reconstituted (−::+, CFG679); *C. auris* – wildtype (+, CFG552), *gdh2* (−, CFG586), reconstituted (−::+, CFG699).

evade fungal killing through modulation of phagosomal pH (Kasper et al., 2014). Like in our previous data in *C. albicans*, *GDH2* is also dispensable for survival of *C. glabrata* during co-culture with macrophages (Figure 5e). As for *C. auris*, we also tested the capacity of wildtype and *gdh2* cells to kill cells in an epithelial monolayer but we are unable to observe any difference between the two (Figure 5f), corroborating previous data that *C. auris* is not cytotoxic to intact skin epithelial cells or epidermis tissue (Brown et al., 2020). In addition, despite amino acid metabolism being implicated in antifungal tolerance (McCarthy & Walsh, 2018), the loss of *GDH2* did not affect the fluconazole susceptibility of either *C. auris* or *C. glabrata* (Figure 5g). In summary, although Gdh2 is the key enzyme that endows *Candida* spp. the capacity to neutralize the environment when grown in amino acids, it remains dispensable for properties associated with virulence.

2.6 | Environmental alkalization does not antagonize growth of *Lactobacillus*

The intriguing finding that inactivation *GDH2* does not affect *C. albicans* virulence (Kasper et al., 2014) motivated us to question the role of environmental pH modulation as a means to alter the composition of the host microbiome. In line with its opportunistic character, it is possible that *C. albicans*-dependent alkalization contributes to create imbalances in the host microflora antagonizing the growth of other competing, and potentially antagonistic microorganisms. For example, *Lactobacillus* species normally inhabit the acidic vaginal microenvironment in most healthy females, and these bacteria are thought to provide protection against *C. albicans* (Wang et al., 2017). Acute vulvovaginal candidiasis (VVC) occurs at least once in the lifetime of most women (75%) and represents a prime example of dysbiosis within a complex host niche (Sobel et al., 1998). Among the *Lactobacillus* species, *L. crispatus* is one of the predominant species in the vaginal tract (Antonio et al., 1999) and is thought to exert the most potent antimicrobial activity against *C. albicans* (Wang et al., 2017), making it an ideal representative of this genus. To experimentally address the possibility that *C. albicans*-dependent alkalization inhibits the proliferation of *L. crispatus* we used a transwell (0.4 μm) culture system schematically depicted in Figure 6a. The *C. albicans* strains were seeded into the transwell at a relatively high starting cell density (~1.6×10^7 CFU/transwell) to minimize growth-dependent effects. The high fungal cell density used was intended to simulate a worst-case scenario where there is a *Candida* overgrowth in VVC. The high fungal density was also used to ensure that the alkalization process would take effect within a reasonable timeframe.

We used a modified alkalization medium (CNY; see Methods) containing ~5.6 mM (0.1%) glucose, which is comparable to the level observed in vaginal secretions (Ehrstrom et al., 2006). Under these conditions, CNY supports the growth of *L. crispatus* and *C. albicans*. We were unable to use MRS medium, commonly used in culturing lactobacilli, due to its high level of glucose (2%), which inhibits alkalization in *C. albicans*, i.e., precisely the parameter under study. The initial pH (pH = 4) is comparable to the acidic vaginal pH, the physiological consequence of lactobacilli-dependent fermentation. Under aerobic conditions, *L. crispatus* failed to grow without *C. albicans* growing in the transwells; *C. albicans* apparently depletes oxygen in the media, a requisite for *L. crispatus* growth (Figure S3A). We deliberately used the non-filamenting *C. albicans* strains carrying null alleles of *CPH1* and *EFG1* (*cph1*Δ/Δ *efg1*Δ/Δ) to exclude potential inhibitory factors associated with filamentation (e.g., candidalysin). The *cph1*Δ/Δ *efg1*Δ/Δ strain is as capable as wildtype in alkalinizing the medium (Figure S3B).

As expected, and in contrast to the *cph1*Δ/Δ *efg1*Δ/Δ strain, the strain lacking *GDH2* (*cph1*Δ/Δ *efg1*Δ/Δ *gdh2-/-*) was unable to alkalinize the media (Figure 6b; Silao et al., 2020). The tight dependency of alkalization on respiration was clear (Figure 6c); under aerobic and microaerophilic conditions, the medium became alkaline in a Gdh2-dependent manner, whereas consistent with the requirement of mitochondrial function, alkalization did not occur under anaerobic conditions. Contrary to our expectations and despite obvious difference in extracellular pH, there were no significant differences in the number of *L. crispatus* cells recovered in the wells with transwells seeded with either *GDH2* or *gdh2 C. albicans* strains (Figure 6d). Also unexpectedly, *L. crispatus* failed to counteract the alkalization exerted by *GDH2* strain grown under aerobic and microaerophilic conditions, which is surprising given that lactobacilli are thought to play a prominent role in maintaining the acidic vaginal pH (Miller et al., 2016) and that *L. crispatus* inhibits growth of *C. albicans* (Wang et al., 2017). Taken together, these results clearly suggest that active pH modulation exerted by *C. albicans* may not effectively antagonize the growth of competing microorganism such as lactobacilli.

3 | DISCUSSION

The interest in studying environmental alkalization as a consequence of amino acid metabolism in *C. albicans* is due its purported link facilitating virulent growth (reviewed in: Fernandes et al., 2017; Miramon & Lorenz, 2017; Vylkova, 2017). A precise understanding of the mechanisms underlying alkalization has remained elusive due to the lack of information regarding how ammonia is generated. *C. albicans* lacks the enzyme urease, which in many pathogenic microorganisms catalyzes the breakdown of urea to ammonia and carbon dioxide (Navarathna et al., 2010). Consequently, urea amidolyase (Dur1,2), which catalyzes the analogous reaction in *C. albicans*, but in two steps, was initially considered to be a primary source of ammonia. However, the inactivation of *DUR*1,2 was found to have a modest effect on alkalization (Silao et al., 2019; Vylkova et al., 2011). We recently discovered that the cytoplasmic glutamate dehydrogenase (Gdh2) is the key enzyme catalyzing the release of ammonia and functions as the major driver of environmental alkalization (Silao et al., 2020). With this

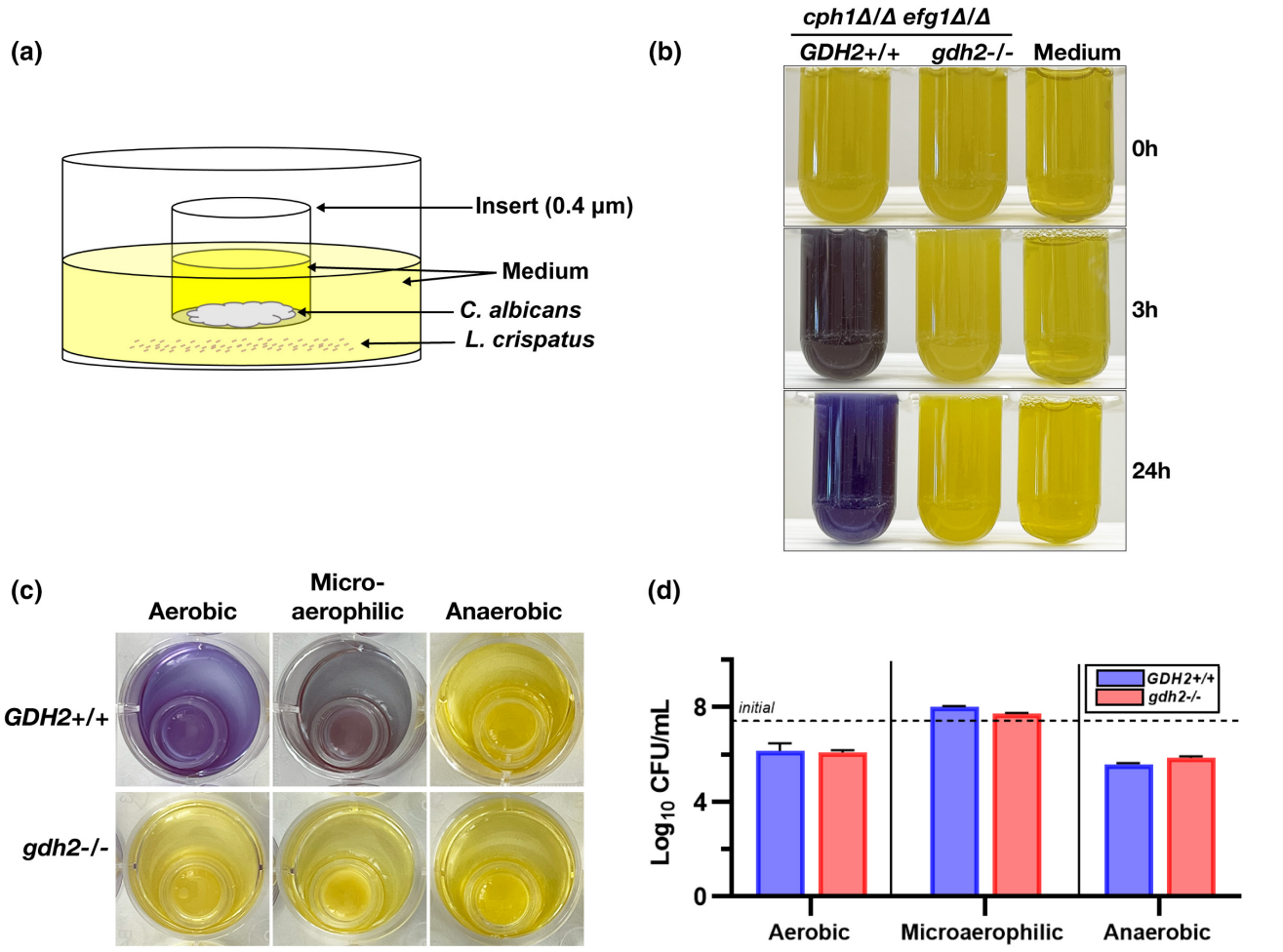

FIGURE 6 Environmental alkalization does not antagonize growth of *Lactobacillus crispatus*. (a) Schematic diagram showing the in vitro set-up to investigate the effect of pH modulation in growth of *L. crispatus*. (b) *cph1*Δ/Δ *efg1*Δ/Δ *GDH2*+/+ (CASJ041) and *cph1*Δ/Δ *efg1*Δ/Δ *gdh2*−/− (CFG352) were grown in CNY alkalization medium at OD ≈ 5 and photographed at the indicated timepoints. (c) Alkalization is dependent on oxygen tension. Photographs of the wells after 48 h of growth under aerobic, microaerophilic, and anaerobic growth conditions. (d) Fungal-driven pH modulation does not antagonize *L. crispatus*. Viable cell counts of *L. crispatus* recovered in the medium indicated in (c); Results ($n = 4$) between *GDH2*+/+ and *gdh2*−/− in each oxygen tension condition were not significant by student *t*-test.

FIGURE 7 Integrative model of amino acid-dependent alkalization of the extracellular growth environment by *Candida albicans*. A) A plot showing the relative concentrations of ammonia (NH_3) and ammonium (NH_4^+) in aqueous solution based on pH set at 37°C. Values were calculated using pKa = 8.89 (Erickson, 1985). The ratio of NH_4^+ to NH_3 in this mixture is highly pH-dependent. (b) Schematic diagram showing the difference in the ammonia release in liquid and solid media. In comparison to solid media, volatile ammonia is more efficiently captured by the acidic liquid culture to form ammonium resulting in a more rapid alkalization of the media. (c) Regulatory control of alkalization gene expression and glutamate-dependent metabolism determines the alkalization potential of *C. albicans*. When cells are shifted from high glucose medium (e.g., YPD) to alkalization medium (e.g., YNB + CAA), *C. albicans* cells are relieved of glucose repression (1) transcriptionally mediated by Mig1/2 repressors binding upstream repressing sequences (URS_{glu}) (2). Cytosolic proline (Pro_{cyto}) enters the nucleus (Pro_{nuc}) where it binds and activates the transcription factor Put3 at upstream activating sequence (UAS_{pro}) (3). In parallel, the transcription factor Stp2 is proteolytically activated by the SPS sensor (Ssy1-Ptr3-Ssy5) in response to extracellular amino acids (4). The processed form of Stp2 efficiently targets the nucleus and binds UAS_{aa} (5). The coordinated activities of these factors determine the transcriptional output of the key alkalization genes (6). Uptake of extracellular amino acids is facilitated by amino acid permeases (AAP) (7). Many amino acids are converted to glutamate in the cytosol (Glu_{cyto}) by transamination reactions (8) that require α-ketoglutarate (α-KG) as a substrate. Proline, enters the mitochondria via an unidentified (?) transporter (9) where it is converted by the proline catabolic pathway (Put1 and Put2) to glutamate (Glu_{mito}) (10). It is postulated that Glu_{mito} is directly or indirectly (?) exported out of the mitochondria (11) and contributes to the Glu_{cyto} pool. This multi-step path involves conversion of Glu_{mito} to aspartate in the mitochondria (Asp_{mito}), predicted to be catalyzed by the mitochondrial aspartate aminotransferase (Aat1). Asp is exported to the cytosol where it gets converted to Glu_{cyto} by cytosolic aspartate aminotransferase. Glu_{cyto} is the substrate of Gdh2 forming α-KG and ammonia (NH_3) (12). Due to the cytosolic pH, maintained at around 6.5 (Rane et al., 2019), the bulk of ammonia rapidly converts to ammonium (NH_4^+). Ammonium is a substrate of central nitrogen metabolism (Gdh3 and Gln1) (13). NH_3, although a minor species, can efficiently diffuse across the cell membrane (14) where it forms NH_4^+ and thereby effectively contributes to neutralizing the extracellular space (15). As the extracellular pH increases, Gdh2 level decrease, and a fraction of Glu_{cyto} is extruded transiently (Glu_{ext}) by a still uncharacterized (?) exporter (17). Glu_{ext} is reassimilated after transport into cells via AAP (18).

knowledge, we assessed the contribution of other factors that impinge on this process and have defined several control points. Based on our findings, we have developed an integrative model that accounts for how the catabolism of amino acids leads to environmental alkalization (Figure 7). Despite its role in alkalization, *GDH2* is dispensable for virulence of *C. albicans* in *Drosophila* and murine models of candidemia (Silao et al., 2020) and in human whole blood (our unpublished results). Our results challenge several commonly accepted dogmas regarding the role of alkalization in fungal virulence.

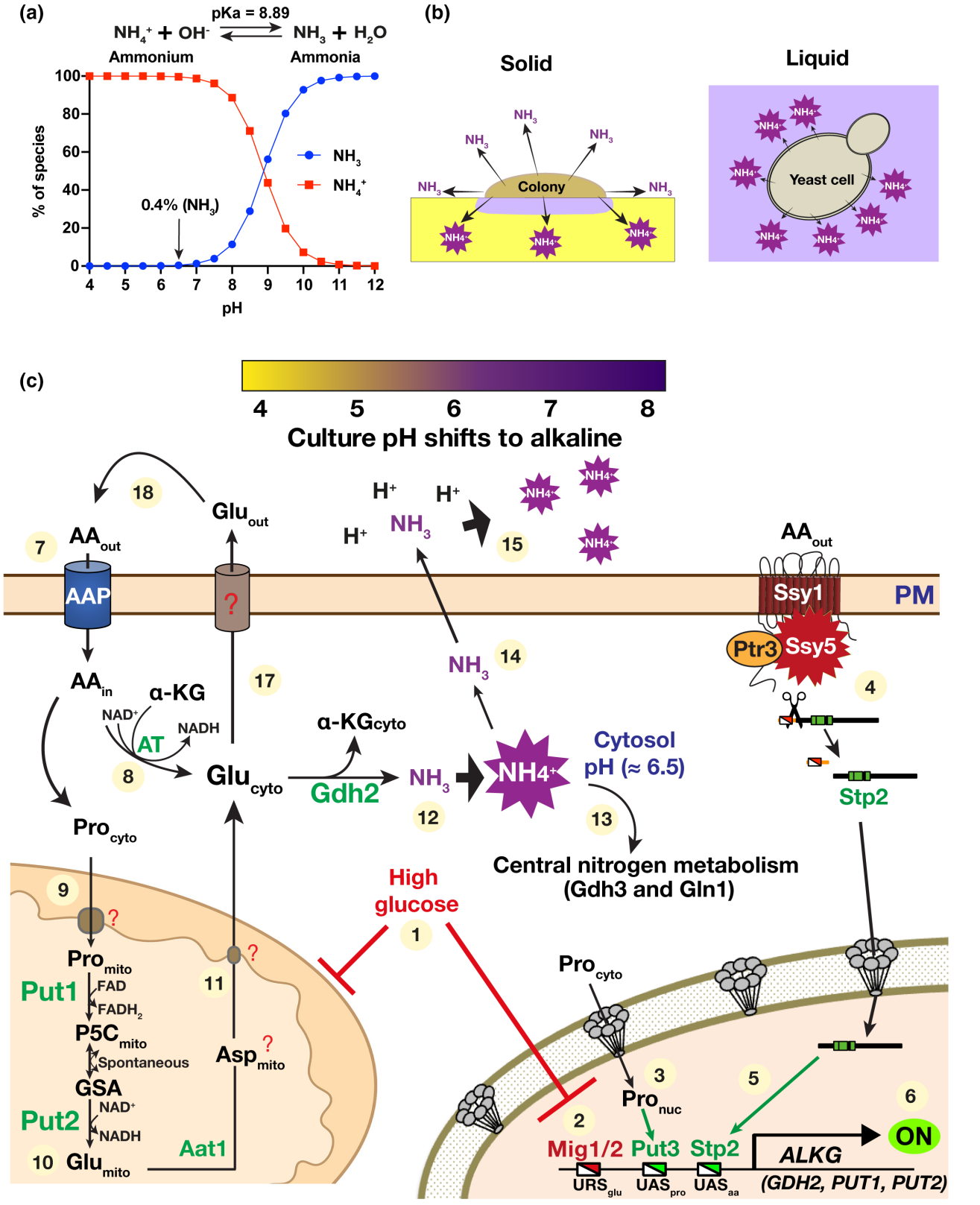

Based on the pK_a of ammonium/ammonia (NH_4^+/NH_3) relationship in aqueous medium (Figure 7a), the ammonia generated by Gdh2 in the cytosol (pH ~ 6.5, Rane et al., 2019) is expected to rapidly form ammonium. Ammonium can be reassimilated by NADPH-dependent glutamate dehydrogenase (Gdh3; α-ketoglutarate to glutamate) and/or glutamine synthetase (Gln1; glutamate to glutamine; Silao & Ljungdahl, 2021). However, it is unlikely that these anabolic reactions can accommodate the amount of excess ammonium generated when cells are metabolizing amino acids as energy sources. Rather, our data are consistent with the notion that ammonia, although present in small amounts (~0.4%), passively diffuses across the cell membrane into the extracellular environment where it contributes to neutralizing the acidic pH. This occurs without needing a dedicated exporter (Antonenko et al., 1997; Cueto-Rojas et al., 2017; Labotka et al., 1995). We tested the role of Ato5, a putative ammonia transport protein, by creating an *ato5*−/− strain. Contrary to previous reports (Danhof & Lorenz, 2015; Vylkova et al., 2011), we were unable to confirm a major effect on alkalization (Figure S2A,B); thus, we excluded Ato5 from our model.

The passive diffusion of ammonia fully accounts for the observed density-dependent alkalization; higher cell densities result in more ammonia released and faster alkalization. This also explains why liquid cultures, rather than colonies growing on solid substrates, exhibit more rapid alkalization. The volatile ammonia (NH_3) formed by colonies diffuses in multiple directions limiting the amount that is directly captured by the solid growth medium (Figure 7b). The use of dense liquid cultures enables the assessment of the alkalization capacity of strains in a manner that is less dependent on growth, e.g., the *nuo1*Δ/Δ strain (Figure 2e). In fact, dense liquid cultures (OD ≈ 5) provides the most conclusive test to rigorously define the involvement of components thought to contribute to alkalization. To our knowledge, Gdh2 is the only component that clearly passes this test, i.e., strains lacking Gdh2 activity exhibit an absolute inaptitude to alkalinize amino acid-based media.

Although Gdh2 is a cytosolic component (Silao et al., 2020, 2023), our model accounts for the tight dependence of alkalization on mitochondrial function (Figure 7c). The substrate glutamate originates primarily from metabolic events in the mitochondria (Figure 2b,c). Consistently, conditions that downregulate mitochondrial function, such as growth in high glucose (2%), limiting oxygen (Figures 2f and 5c), the lack of mitochondrial respiratory subunits (*nuo1*Δ/Δ), or inhibition by Antimycin A, all result in alkalization deficiency. Indeed, regardless of how amino acids are used by the cells, i.e., as sole carbon/nitrogen/energy source (YNB + CAA), as sole nitrogen source (YNB + CAA supplemented with 1% glycerol, 1% lactate, or <0.2% glucose as main carbon sources), or as a supplementary carbon/nitrogen/energy sources (YNB + CASG), alkalization readily occurs as long as the conditions permit respiratory growth, which enables the steady supply of mitochondrial glutamate to the cytosol to support the intrinsic catalytic activity of Gdh2. High glucose represses mitochondrial function and Put1 and Put2 expression, thus lowering intracellular glutamate (Figure 2a). The coupling of reduced intracellular glutamate with the downregulation of mitochondrial function explains why alkalization is virtually abolished in high glucose. Strains lacking *PUT1* and *PUT2* exhibit delayed alkalization even in dense cultures (Silao et al., 2019, 2020), but alkalization is ultimately achieved presumably due to multiple transamination reactions that generate glutamate (Silao & Ljungdahl, 2021). We note that high glucose-mediated repression of the mitochondrial function can result in the generation of fermentation by-products and CO_2, which can contribute to maintaining acidic pH (Morales et al., 2013; Silao et al., 2019). We predict (Figure 7c) that glutamate can be directly exported out of the mitochondria by a dedicated transporter, or alternatively, after being converted to aspartate (or other amino acids via transamination). These represent two distinct mechanisms, and dissecting them will require efforts that go beyond the scope of this work.

We traced the prominent alkalization defect of strains carrying *stp2* to the inability to fully derepress *GDH2*, *PUT1*, and *PUT2* (Figure 4). This is consistent with, but adds to our recent findings (Silao et al., 2023) that the proline-dependent expression of Put1, Put2, and Gdh2 is partially independent on Put3. The additive effect of combining *stp2* and *put3* mutations indicate that Stp2 and Put3 function in parallel to regulate the enzymes contributing to alkalization in *C. albicans*. This relationship explains some of the interesting *stp2* phenotypes that are relevant to *C. albicans* pathogenesis, such as the defective filamentation in the phagosomes of macrophages (Danhof & Lorenz, 2015; Vylkova & Lorenz, 2014) and virulence in murine systemic infection model (Amorim-Vaz et al., 2015; Vylkova & Lorenz, 2014), which we have also shown to be dependent on proline catabolism (Silao et al., 2019, 2023). The data presented here also help explain other findings related to the increase in proline uptake in *stp2* mutant (Bottcher et al., 2022), which is likely a compensatory mechanism to generate more energy when intracellular amino acids become limiting. The tight dependency of Gdh2 expression on Stp2 represented an apparent conundrum given that Gdh2 expression is extremely low in YPD (Silao et al., 2020) even though Stp2 is constitutively expressed and activated (Martinez & Ljungdahl, 2005; Miramon & Lorenz, 2016). However, this can be understood since *GDH2* expression is apparently subject to glucose repression by Mig1 and Mig2; these factors have been shown to negatively regulate *GDH2*, *PUT1*, and *PUT2* (Lagree et al., 2020). Shifting cells from YPD to YNB + CAA medium with low glucose relieves the repression, presumably enabling Stp2 and Put3 to activate expression of target genes by binding to putative UAS_{aa} and UAS_{Put3} in their promoters. Also, the level of Gdh2 is tightly regulated; its levels rapidly decrease as pH increases, whereas the levels of Put1 and Put2 do not (Figure 1). Further work is required to experimentally define the precise nature of the promoter regions in these genes. For example, since Gdh2 is weakly expressed in YNB + CAA with 2% glucose (Figure 2b), glucose repression cannot fully explain the lack of Gdh2 expression in YPD grown cells (Silao et al., 2020). In addition,

whether Stp2 regulates *GDH2*, *PUT1*, and *PUT2* by directly binding to their indicated promoter regions (Figure 4d) or indirectly through regulation of an intermediate transcription factor needs to be further examined.

The observation that Gdh2 levels decrease as the extracellular pH increases and cells extrude glutamate suggests that cells do this to limit ammonia production and thereby actively respond by reducing the negative consequences of creating an alkaline growth environment. A similar strategy has been demonstrated in *S. cerevisiae*, which limits the production of ammonia by excreting amino acids, including glutamate via transporters that belong to the multidrug resistance transporter family postulated to function as H^+ antiporters (e.g., Aqr1) (Velasco et al., 2004). We note that the *C. albicans* genome encodes a putative *AQR1* homolog (*QDR2*/C3_05570W); however, we have not investigated if it operates similarly to *S. cerevisiae*. We found that the extrusion of glutamate by *C. albicans* is transient as the excreted glutamate is eventually reassimilated. It is unclear whether other amino acids are also excreted in addition to glutamate, but it would not be surprising if there are others. At this point, defining the precise transport processes will involve more experimental work. The fact that *C. albicans* extrudes glutamate, which reduces the alkalization potential, suggests that as other fungi, they prefer acidic growth conditions that provide a competitive advantage over many bacteria, is more favorable to facilitating nutrient uptake powered by the proton gradient, and minimizes the potential loss of nitrogen. Finally, maintaining an acidic growth environment likely contributes to keeping intracellular ammonium levels below toxic levels. Ammonia, not ammonium, readily diffuses across the plasma membrane (Antonenko et al., 1997; Cueto-Rojas et al., 2017; Labotka et al., 1995) in a direction toward a lower pH, effectively pulling the ammonium/ammonia equilibrium to drive excess ammonium out of cells.

As in *C. albicans*, Gdh2 is essential for the growth of *C. glabrata* and *C. auris* in media with amino acids as the sole carbon/nitrogen/energy source (YNB+CAA). We exploited this phenotype during strain constructions (Figure 5a). Consistent with our finding that Gdh2 is dispensable for *C. albicans* virulence (Silao et al., 2020), *GDH2* appears also to be dispensable for virulence of both *C. glabrata* and *C. auris*, as assessed by survival in a whole human blood, and in other more specific virulence model such as macrophages (for *C. glabrata*) and epithelial cells (for *C. auris*). We anticipated the results observed for *C. glabrata* given that *C. albicans*, which show more robust alkalization capacity than *C. glabrata*, failed to alkalinize an acidic phagosome (Silao et al., 2020). This is entirely consistent to the V-ATPase pumping rate calculated by Westman et al., which is several orders of magnitude higher than the capacity of *C. albicans* to extrude ammonia (Westman et al., 2018). It is unlikely that *C. glabrata* can exert any significant change in phagosomal pH through ammonia production. The fact that Gdh2 is dispensable for virulence indicates that the metabolism of other carbon sources suffices for growth of *gdh2* strains within the model host systems tested. The apparent difference in the virulence of *put* and g*dh2* mutants can be attributed to the toxicity exerted by proline in strains that are unable to catabolize it, i.e., proline inhibits mitochondrial function in *put1* and *put2* mutants (Silao et al., 2023), a phenotype that is not observed in *gdh2* mutants.

Alkalization has been speculated to generate conditions that favor disease-associated vaginal microbes, providing opportunities for *Candida* overgrowth (Vazquez-Munoz & Dongari-Bagtzoglou, 2021) and access to host epithelial cells (van de Wijgert et al., 2014). We initially considered applying a murine vaginal infection model to critically test prevailing notions regarding the importance of fungal-induced alkalization. However, contrary to the acidic human vaginal pH, the murine vaginal pH is near neutral (Miao et al., 2021). Consequently, the murine vaginal model is not well-suited to assess the significance of alkalization. This realization prompted us to develop a transwell assay (Figure 6) to specifically test whether the capacity of *C. albicans* to increase the extracellular pH negatively affects the growth of lactobacilli that comprise roughly 70% of the human vaginal tract microbiome. This contrasts to non-human primates, including rodents, where lactobacilli comprise <1% of the vaginal tract microbiome (Miller et al., 2016). The use of *L. crispatus* as a representative *Lactobacillus* species was deliberate given its potent antifungal character (Jang et al., 2019; Wang et al., 2017). The observation, that despite robust growth under aerobic and microaerophilic conditions, *L. crispatus* was unable to counteract the alkalization by *C. albicans* in a culture medium containing low but physiological levels of glucose (0.1%) requires comment. First, fungal-induced alkalization did not inhibit *L. crispatus* growth, making it unlikely that fungal-induced alkalization, per se, significantly impairs the growth of resident lactobacilli in the vaginal tract. Second, *C. albicans* supported the growth of *L. crispatus*, a strict anaerobe, under aerobic conditions, presumably by sequestering oxygen. These data are consistent with reports of vaginal yeast colonization within *Lactobacillus*-dominant vaginal microbiomes (Eastment et al., 2021; van de Wijgert et al., 2014). Third, although this experimental set-up does not take into account alternative carbon sources, it is reasonable to expect that *Lactobacillus* spp. ferment other carbohydrate sources, e.g., glycogen, to maintain an acidic vaginal pH (Wang et al., 2017). Fourth, based on our finding that fungal-driven alkalization is strictly coupled to respiration (Figures 2f and 6c), the vaginal microenvironment is likely to be oxygen-limiting. Thus, even if there are transient increases in oxygen tension and pH, and also the influx of nutrients associated with increased sexual activity and menstruation (Alvarez et al., 2015; Ng et al., 2018; Wagner et al., 1984; Wagner & Levin, 1978), it is unlikely that *C. albicans* contributes directly to long-term alkalization of the vaginal tract. Our findings align with clinical observations that in contrast to vaginitis caused by bacteria or *Trichomonas*, vaginal candidiasis is not associated with an increase in vaginal pH (Lin et al., 2021). Rather it is likely that other fungal-associated processes are more critical in diminishing the efficacy of the mucosal barrier and of the vaginal microbiome to restrict fungal growth and limit access to epithelial cells.

Lactobacilli, especially *L. crispatus*, are known to strongly inhibit *C. albicans* hyphal formation (MacAlpine et al., 2021; Wang et al., 2017); hyphae facilitate invasion and damage of epithelial cells, which stimulates the release of pro-inflammatory cytokines and chemokines that trigger host immune response (Moyes et al., 2016; Netea et al., 2015; Richardson, Ho, et al., 2018; Richardson, Willems, et al., 2018). *Lactobacillus*-mediated inhibition of *C. albicans* hyphal formation has been traced to the secretion of 1-acetyl-β-carboline (1-ABC), a small molecule that inhibits Yak1, a member of the dual-specificity tyrosine phosphorylation-regulated kinase (DYRK) family (MacAlpine et al., 2021). Consistent with current understanding, we have observed that spent media from *L. crispatus* inhibits *C. albicans* growth (data not shown). However, in the context of our transwell co-culture experiments, although *L. crispatus* grew in the microaerophilic conditions, and presumably secrete normally, *C. albicans* retained the capacity to alkalinize the media, indicating that mitochondrial functions remain intact. The failure to counteract the alkalization by *C. albicans* indicates that the inhibitory effects of *L. crispatus* toward *C. albicans* does not appear to involve mitochondrial repression in a manner analogous to the effect of phenazine produced by *Pseudomonas aeroginosa* (Morales et al., 2013). To conclude, although alkalization is not directly required for virulence of *C. albicans* and other *Candida* spp., the results reported here warrant the reassessment of virulence processes reportedly linked to or associated with pH modulation by fungal pathogens. Our future efforts will examine how *Candida* cells adjust their metabolism in the context of infection, which we posit involves transcriptional and/or translational arrest.

4 | METHODOLOGY

4.1 | Organisms and culture

All key materials (organisms, chemicals, oligonucleotides, and software) used in this work are summarized in Table S1 (Key resource table). Yeast strains were routinely cultivated on YPD agar (1% yeast extract, 2% peptone, 2% glucose, and 2% Bacto agar) following recovery from glycerol stock stored in a −80°C freezer. Where needed, YPD is supplemented with nourseothricin (Nou) at the required concentrations (200-, 100-, and 25-μg/mL) from filtered stock (200 mg/mL). Overnight YPD broth cultures were prepared by picking single colonies from a YPD plate and grew in a shaking incubator (Infors HT Multitron Incubator Shaker) set at 30°C and 150–180 rpm. Alkalization was routinely assessed using the standard YNB + CAA medium (0.17% yeast nitrogen base without amino acids and ammonium sulfate (YNB), 1% of casamino acids (CAA) containing 0.01% Bromocresol Purple (BCP) as pH indicator. CAA, derived from the controlled acid hydrolysis of casein, contains free amino acids and oligopeptides at a ratio of 82%–18%, respectively (Hebert et al., 2008). This medium and other alkalization media were adjusted to pH = 4.0 using 1 M HCl before sterile-filtered (0.45 μm). The base medium was used without or with 2% glucose depending on the experiment. Where indicated, YNB + CAA is supplemented with 38 mM ammonium sulfate (5 g/L ≈ 38 mM) and 1% glycerol (YNB + CASG) to support the growth of some mutants, or used without BCP. For glutamate extrusion analysis, YNB was supplemented with 0.5 g/L each of Proline, Arginine, Leucine, Alanine, and Aspartate, and added with 1% Glycerol as the main carbon source, which is referred elsewhere in the text as YNB + PALAAG medium and used without BCP. For the alkalization experiment with *Lactobacillus crispatus*, the CNY medium was composed of YNB (0.085%), CAA (0.5%), proteose peptone no. 3 (0.375%), yeast extract (0.095%), NaCl (0.125%), glucose (0.1%), BCP (0.01%); this medium is a 50:50 mix of standard YNB + CAA medium and NYCIII medium (without glucose) and then supplemented with glucose and BCP at the indicated concentrations. Other specific media modifications are indicated elsewhere in the text. Stock solutions of different carbon and nitrogen sources used are as follows: glucose (40%), glycerol (20%), and ammonium sulfate (1 M).

4.2 | CRISPR/Cas9 gene editing

For inactivation of *STP2*, the pV1524 vector bearing the *STP2* 20-bp sgRNA (pFS136, derived from primers p6/p7), repair templates (RT) with in-frame stop codon and *Xho*I restriction site (p8/p9), and verification primers (p10/p11) can be found in Table S1. For *ATO5* inactivation, two sgRNAs were designed corresponding to pFS141 (p12/p13) and pFS143 (p14/p15). Since these sgRNA regions are in close proximity, a common set of RT (p16/p17) and verification primers (p18/p19) were used for both. The *PUT3* vector (pFS084), RT (p2/p3), and verification primers (p4/p5) were previously described (Silao et al., 2019). Specific sgRNAs were cloned in either pV1093 (*PUT3*) and/or pV1524 (*STP2 or ATO5*) by blunt-end ligation. Cassettes were verified by sequencing using primer p1 and then released by digestion with *Kpn*I/*Sac*I (5 μg plasmid/digestion). Digested cassettes and RTs (generated by template-less PCR) were PCR-purified and co-transformed into the indicated strain using the hybrid lithium acetate/DTT-electroporation method, as previously described in (Silao et al., 2019). Nourseothricin-resistant (Nou^R) transformants were selected on YPD + 200 μg/mL Nou, and further clonal purification was made on YPD + 100 μg/mL Nou. Transformants were purified and verified several by colony PCR using the appropriate primers to amplify the mutated gene and then digested with *Xho*I to identify the knockouts. For pV1524-derived plasmids, cassette excision was done by growing purified colonies in liquid YPM and then plating on YPD + 25 μg/mL Nou. Nourseothricin-sensitive (Nou^S) pop-outs were verified by streaking on YPD + 100 μg/mL Nou. For the construction of *stp2−/− put3−/−* double knockout strain, the Nou^s *stp2−/−* strains were co-transformed with the digested pFS084 and RT, and transformants were selected accordingly. In most cases, single preparations of purified digested cassettes and RT sufficed for 10–15 independent transformations and were kept at −20°C until used.

4.3 | Genetic construction of *gdh2* and reconstituted *C. glabrata* and *C. auris* strains

Since *C. glabrata* and *C. auris* are haploids, a homology-directed recombination gene deletion strategy was used to delete *GDH2* in these strains. Briefly, a knockout cassette was amplified from an HA-tagging plasmid (pFS069 = pFA6a-3HA-SAT flipper; Silao et al., 2019) using primer pairs p21/p22 for *C. glabrata GDH2* (CAGL0G05698g) and p28/p29 for *C. auris GDH2* (B9J08_004192). pFS069 was derived from the original *SAT1*-flipper cassette (Reuss et al., 2004). This tagging cassette has a very good recombination efficiency even if the homology flanking regions to the target genes are short (<100-bp). Amplified cassettes were purified and transformed into *C. glabrata* (ATCC 2001) and *C. auris* (CFG552) wildtype strains and Nou^R transformants selected on YPD + 200 μg/mL Nou. Purified colonies were checked for correct integration, and verified knockouts were stored at −80°C as glycerol stock without removing the NAT^R marker, as it would be used as a marker for reconstitution. The following primers were used to verify junctions for correct knockout cassette integration: *Cg-gdh2*Δ (p27/p24; p23/p34) and *Cau-gdh2*Δ (p27/p30; p33/p34). For genetic reconstitution of knockout strains, a region of the *GDH2* gene was amplified by PCR from the respective wildtype strains using primers p25/p26 for *C. glabrata GDH2* and p31/p32 for *C. auris GDH2*. The amplicons were purified and then transformed into the respective knockout strains. Electroporated cells were recovered in YNB + CAA medium for 6–8 h and then plated on YNB + CAA agar. Plates were incubated for 2–3 days at 30°C until colonies appeared. These colonies were purified on YPD, and then 3–5 independent colonies per transformation were tested for correct integration by PCR (*C. glabrata*, p23/p24; *C. auris*, p33/p30) and restriction digest using either *Xho*I (*C. glabrata*) or *Apa*I (*C. auris*). The verified reconstituted strains were tested for growth on YPD agar with 200 μg/mL nourseothricin to determine the loss of the Nou^R marker, indicating replacement by the reconstituted allele.

4.4 | Alkalization assay

For routine assays, single colonies from YPD plates were picked and grown overnight (16–20 h) in YPD broth and then collected the following day by centrifugation at 4000 *g* for 3–5 min. Depending on the number of cells needed, overnight cultures were prepared in 3-, 25- or 50 mL volumes. Harvested cells were washed twice with ddH_2O and then resuspended in ~20% of the original culture volume to concentrate the cells. Optical density (OD) at 600 nm was measured, and used this value to inoculate prewarmed YNB + CAA or YNB + CASG medium (37°C) at OD ≈ 0.1, 2, or 5. Where indicated, YNB + CAA medium was supplemented with 2% glucose. Cultures were incubated in a 37°C shaking incubator (150–180 rpm), and depending on the experiment and specific timepoints, cultures were photographed and/or sampled for further analysis. Where needed, the pH of the culture was measured using a table top pH meter (pH 1100 L; VWR, Sweden).

For determination of alkalization potential (ΔpH) as a function of starting pH (pH_i), cells from YPD pre-culture were inoculated into a 50 mL standard YNB + CAA (pH = 4) medium at OD ≈ 2 and then grown for 2 h at 37°C to express Gdh2. Cells were then collected by centrifugation (4000 *g*, 5 min, room temperature; SL 40R, Thermo Scientific) and the medium removed by decanting. Excess medium was removed by pipetting following a quick centrifugation step. Cell pellets were thoroughly resuspended in sterile ddH_2O and then aliquots of equal volume were inoculated into baffled flasks containing 25 mL of YNB + CAA medium adjusted to pH = 4 or 6. Cultures were incubated for 3 h at 37°C and then the resulting pH (pH_{3h}) determined. ΔpH was calculated by subtracting pH_i from pH_{3h}. It is noted that the addition of cell aliquots into the culture medium did not affect pH_i.

4.5 | Enzyme expression analysis

A 1 mL aliquot of the culture at 2 h timepoint prepared from a starting OD ≈ 2 was immediately mixed with 250 μL of cold 2 M NaOH with 7% β -mercaptoethanol (βME) to lyse the cells. After 15 min, an equal volume of 50% trichloroacetic acid (TCA) was added to precipitate the proteins, which was carried out overnight at 4°C. Protein pellets were harvested by high-speed centrifugation (17,000 *g*, 10 min, 4°C) and then the residual liquid in the tube completely removed by a quick high-speed spin. Protein precipitates were solubilized completely in a 50 μL 2X SDS sample buffer containing 5% βME and 167 mM of Tris Base (pH ≈ 11) and then boiled at 95°C for 5 min. Proteins were resolved in 4%–12% Bis-Tris pre-cast gel using either MES or MOPS buffer and then subjected to a standard immunoblotting procedure in a nylon membrane. After transfer, membranes were blocked using 10% skimmed milk in TBST (TBS + 0.1% Tween) for 1 h at room temperature. Target proteins were detected individually or simultaneously using an optimized antibody cocktail prepared in 5% skimmed milk in TBST for both primary (α-GFP (1:3000), α-mCherry (1:6000), α-Tdh3 (1:5000), α-actin (1:5000) α-tubulin-HRP (1:10000)), and secondary (goat α-mouse poly-HRP (1:15000), goat α-rabbit poly-HRP (1:15000), α-HA-HRP (1:15000)). When used in a cocktail, α-tubulin-HRP (1:10000) was added fresh to the secondary antibody as it is already conjugated to HRP. A chemiluminescent substrate (SuperSignal Dura West Extended Duration Substrate) was added to detect immunoreactive bands in blots using the Azure detection system.

4.6 | Cycloheximide (CHX) treatment

Cells collected from YPD cultures were inoculated into 20 mL of YNB + CAA at OD ≈ 2 and then grown continuously with shaking at 37°C. After 2 h, 3 mL culture aliquots were added to separate tubes containing concentrated buffers (500 mM, pH = 4–8) diluted by cultures to 50 mM final concentration. After brief mixing, CHX was added to each tube at 200 μg/mL final concentration and then

incubated for another 1 h at 37°C before taking an aliquot for cell lysate preparation using the NaOH/TCA method (see preceding section). For the unbuffered control, an equal volume of ddH_2O was added to the tube, and immediately after adding CHX, a 1 mL culture aliquot was mixed with NaOH/βME solution to prepare cell lysate, which was then used as reference (T = 0 h) for all comparisons. The selection of pH buffers used was based on their buffering capacities: sodium acetate (pH = 4, 5), MES (pH = 6), and HEPES (pH = 7, 8).

4.7 | Glutamate analysis

Following manufacturer's instructions, glutamate levels in cells or spent medium were analyzed in a microplate format using the Glutamate Assay Kit from Abcam (Fluorometric, LOQ ~1 μM; Cat.#ab138883). (i) Total intracellular glutamate. Cells (CFG404) from overnight YPD cultures were harvested, washed, and inoculated in YNB + CAA without or with 2% glucose at OD ≈ 2. After 2 h of growth at 37°C, cells were harvested, washed 3x with ice-cold ddH_2O, and then resuspended in lysis buffer (25 mM Tris–HCl (pH = 7.2), 150 mM NaCl, 5 mM $MgCl_2$, 1% NP-40 (Igepal CA-630), and 5% glycerol) with 1 mM PMSF and cOmplete™ protease inhibitor. Cells were lysed by bead-beating using FastPrep™ (60 s at 6.0 m/s) for 5 cycles with 3 min rest on ice between cycles. Lysates were clarified by centrifugation at 17000 *g* for 10 min at 4°C, and then the supernatant was saved for glutamate analysis, protein content determination, and immunoblotting. Protein content was analyzed by the Bicinchoninic acid (BCA) assay (Sigma). Samples for immunoblotting were added with 2× SDS sample buffer and run. Glutamate and protein measurements were performed in a BioRad (Enspire) microplate reader. (ii) Extracellular glutamate. For glutamate analysis in spent medium, cells from YPD cultures of wildtype (SC5314) and *gdh2−/−* (CFG279) strains were harvested, washed extensively (4x) with excess ddH_2O to remove the residual YPD medium, and then resuspended in ddH_2O. Cells were diluted at OD ≈ 2 in 20 mL of prewarmed YNB + PALAAG medium and then grown in a shaking incubator at 37°C, and then after 3 h or 5 h, a 5 mL aliquot was taken for analysis. Briefly, the cultures were centrifuged at 4000 *g* for 5 min, and then a 3 mL aliquot of the supernatant was removed and filtered (0.2 μm). A 200 μL from this filtered supernatant and the sterile medium were neutralized with 10 μL of 1 M HEPES, pH = 7.4 (50 mM final concentration) to convert all glutamic acids to glutamate. Except for the uninoculated medium, samples were diluted in 50 mM HEPES before subjecting to glutamate analysis. For practicality, samples collected on different days were stored at −80°C until the run. Results presented were derived from 4 to 7 biological replicates performed in duplicates and run in a TECAN microplate reader in two batches (2 different days). (iii) Cytosolic glutamate. To analyze cytosolic glutamate in cells treated with antimycin, we followed the cytosolic extraction protocol by Ohsumi et al. (1988) with minor modifications. Briefly, cells (CFG441) harvested from overnight YPD cultures were washed and then diluted into 20 mL of YNB + CASG at OD ≈ 2. Cultures were grown for 2 h at 37°C. Then, 5 mL aliquots of the culture were transferred into two 15-ml falcon tubes and immediately spiked with either antimycin A (1 μg/mL final concentration) or ethanol (vehicle). Cultures were placed in the 37°C shaker for 30 min, and then the cells were harvested, washed 3×, and resuspended by brief vortexing in 1.5 mL of the extraction buffer [2.5 mM potassium phosphate (pH = 6), 0.6 M sorbitol, 10 mM glucose, and 0.2 mM $CuCl_2$]. Cells were incubated at 30°C for 10 min with gentle shaking (70 rpm) to permeabilize the cell membrane releasing the cytosolic amino acids. After incubation, a 1 mL aliquot was passed through a 0.45 μm filter connected to a syringe to collect the filtrate. An aliquot of the extract was neutralized by adding 1 M HEPES (pH = 7.4) to 50 mM final concentration to convert glutamic acids to glutamate before analyzing for glutamate.

4.8 | Alpha-Ketoglutarate analysis

The cytosolic extracts obtained from antimycin-treated cells (see preceding section) were also analyzed for α-ketoglutarate using the Alpha Ketoglutarate (alpha KG) Assay Kit (Cat. # ab83431) following the manufacturer's instruction. Briefly, aliquots of the extracts were first deproteinated by TCA and then later neutralized with KOH. Neutralized extracts were added with HEPES (to 50 mM final concentration) to ensure the extract pH was around 7.4 during analysis.

4.9 | Fluconazole susceptibility assay

Broth microdilution assay was performed in a microplate format according to the protocol by EUCAST method (Subcommittee on Antifungal Susceptibility Testing (AFST) of the ESCMID, 2008) with minor modifications that are limited to dissolving the fluconazole powder in 2% DMSO solution in ddH_2O and cell density adjustment by OD (1 OD ≈ 3×10^7 CFU/mL). The minimum inhibitory concentration (MIC) is the lowest drug concentration that gives rise to ≥50% growth inhibition of the drug-free control.

4.10 | Ex vivo human whole blood infection

Freshly extracted anonymized blood samples (4 mL) were purchased from Blodcentralen (Odenplan, Stockholm, Sweden), and all investigations were conducted according to the principles expressed in the Declaration of Helsinki. The well-established donation protocol for collecting human blood by the Karolinska University Laboratory for purposes other than medical treatment provided samples of peripheral blood collected from healthy volunteers with explicit consent for use in this study. According to legal requirements, the samples were labeled with donation numbers for traceability, but no names or other personal data was provided. Upon receipt in our laboratory, the samples are de-identified and can no longer be traced to an individual. This study does not require specific ethical approval.

For infection, fungal cells were first grown overnight in YPD and then refreshed the following day in a fresh medium. Exponentially growing cells were collected, washed twice in PBS, and then adjusted to 1×10^7 CFU/mL. Around 1×10^5 cells (10 μL) were added to 400 μL of whole blood (+EDTA), mixed briefly, and then incubated for 1 h in a shaking heat block (Eppendorf) set at 37°C and 400 rpm. After incubation, tubes were vortexed vigorously, serially diluted in ddH_2O (to lyse human cells), and plated on YPD agar. Plates were incubated at 30°C for 2 days and colonies (CFU) counted. % Survival of fungal cells was calculated by comparing the CFU after the 1 h incubation to the CFU of the inoculum.

4.11 | Macrophage co-culture assay

Primary bone marrow-derived macrophages (BMDM) were used to compare the survival of *C. glabrata* wildtype and *gdh2* mutant in macrophages. Briefly, bone marrows collected from mouse femurs of C57BL/6 wildtype mice (7- to 9-week-old) were differentiated in differentiation medium (DM) composed of complete DMEM medium (referred to as D10) supplemented with 20% L929 conditioned medium (LCM) in a humidified chamber set at 37°C with 5% CO_2. D10 is composed of DMEM medium (high glucose) supplemented with 10% fetal bovine serum (FBS), and 100 U/mL penicillin and 100 μg/mL streptomycin. Differentiation was carried out initially in 10 mL of DM for 3 days before boosting the cells with another dose (10 mL) of DM until macrophages are fully differentiated (about 7–10 days after plating). Macrophages were collected by PBS-EDTA treatment followed by gentle scraping. Macrophages resuspended in D10 were seeded in a 48-well dish at 3.5×10^5 cells/well and allowed to adhere overnight. The following day, exponentially growing *C. glabrata* wildtype (ATCC 2001) and *gdh2* (CFG670) strains in YPD cultures were harvested, washed 2X with PBS, and then adjusted to OD ≈ 1 (~3×10^7 CFU/well). A 200 μL aliquot of the cell suspension was removed and then incubated with 1 μL of α-*Candida albicans* antibody (1:200 dilution) for 30 min at 37°C in a tabletop shaker to opsonize the cells. Opsonized cells were first diluted in pre-warmed D10 to ~2.35×10^5 CFU/mL and then a 500 μL aliquot was used to replace the macrophage growth medium to obtain an MOI of 1:3 (C:M). Plates were spun down (300*g* for 3 min) to collect the *Candida* cells at the bottom of the well. The use of low MOI and the extra opsonization step were to ensure that all fungal cells would be phagocytized by macrophages. Co-cultures were performed for 2 h in a humidified chamber at 37°C with 5% CO_2, after which the wells were treated with Triton X-100 to a final concentration of 0.1% to lyse the macrophages and release the fungal cells. Lysates were serially diluted and then plated onto YPD. Survival of *Candida* cells following co-culture (% Survival) were determined by comparing the recovered CFU to the initial CFU.

4.12 | Epithelial cell cytotoxicity assay

Epithelial cells (A375; ATCC CRL-1619) growing to 80%–90% confluency in D10 in a T-25 flask at 37°C with 5% CO_2 were harvested by digestion with 0.5 mL of TrypLE for 5 min at 37°C. Detached cells were mixed with 6 mL of fresh D10 medium to deactivate the enzyme. Cells were then transferred into a 50 mL tube, harvested by centrifugation at 300*g* for 5 min at 4°C, and then resuspended in 6 mL of fresh D10 medium. Viable cells were counted by trypan blue exclusion, diluted to 1×10^6 cells/mL in D10, seeded into 96 well plate at 1×10^5 cells/well, and then allowed to adhere overnight in the humidified incubator. The following day, *C. auris* wildtype (CFG552) and *gdh2* (CFG586) cells from exponential phase YPD cultures were harvested, washed twice with PBS, and then diluted in D10 medium at 3×10^6 cells/mL. To start the infection, the growth medium of A375 was removed using a multi-channel pipette followed by addition of 100 μL aliquots of fungal cell suspensions containing 3×10^5 cells (MOI 3:1, C:M). Plates were centrifuged briefly at 300*g* for 3 min to collect the fungal cells to the bottom of the wells before incubating it for 24 h in the humidified chamber. After incubation, wells were washed with gentle pipetting up and down with sterile PBS repeated five times (5×) to remove fungal cells. After the final wash, 120 μL of complete D10 medium containing resazurin dye (0.025 mg/mL) was added into each well. The plate was incubated in a humidified chamber for 2 h and then the fluorescence measured using a TECAN microplate reader at excitation and emission of 535 and 595 nm, respectively. To measure cytotoxicity, raw resazurin signals from infected and non-infected wells were first subtracted with signals from no cell control wells (with D10 medium only) and then the normalized signal from infected well (IW) were subtracted with signal from non-infected well (NIW) (i.e., cytotoxicity = IW-NIW). To ensure the exact processing across all treated and control wells, a multi-channel pipette was used for all steps. Experimental data were derived from two independently grown A375 cells each infected with at least two independent colonies of the indicated *C. auris* strains, all performed in duplicates.

4.13 | Transwell assay

Lactobacillus crispatus (LC100) vaginal isolate from a healthy female was recovered on MRS agar medium from glycerol stocks and incubated anaerobically for 48 h at 37°C in anaerobic jar (GasPak™) with an Anaerogen sachet (Oxoid). For broth culture, isolated colonies were grown anaerobically in MRS broth for 48 h at 37°C. Cells were then collected by centrifugation 6000*g* and then washed three times to remove the media. Cells were inoculated into CNY medium at ~3×10^7 CFU/mL, and then a 500-μL aliquot (~1.5×10^7 CFU/well) of the suspension was gently dispensed in the well of a 24-well plate containing a sterile insert (Millicell, 0.4 μm PCF, Cat. # PIHP01250; Merck Millipore, Ltd.) placed at the center of the well. For the processing of fungal cells, *cph1*Δ/Δ *efg1*Δ/Δ (CASJ041) or *cph1*Δ/Δ *efg1*Δ/Δ *gdh2*−/− (CFG352) cells were harvested from overnight YPD broth, washed twice in ddH_2O, and then resuspended in CNY medium at OD ≈ 5. A 200 μL aliquot (OD ≈ 1; ~1.6×10^7 CFU/well) was carefully pipetted into the center of the insert. Plates were then incubated in aerobic, microaerophilic, and anaerobic conditions for 48 h at 37°C

before photography and sampling the external culture for viable cell count via plating on MRS agar. All preparations were done in a Don Whitley anaerobic chamber (85% N_2, 10% CO_2, 5% H_2) prior to incubation. Aerobic incubation was done in static, ambient conditions while microaerophilic (6.2–13.2% O_2, 2.5%–9.5% CO_2) and anaerobic (<1% O_2, 9%–13% CO_2) conditions were met using an anaerobic jar with a Campygen sachet (Oxoid) and Anaerogen sachet (Oxoid), respectively.

4.14 | Statistical analysis

Data shown in this work were derived from at least 3 independent biological replicates and were analyzed using GraphPad Prism version 9. Specific statistical treatment applied and error bars used are described in the appropriate figure description and applied to the data obtained. Depending on the experiment, statistical treatments include unpaired student *t*-test or regular one-way analysis of variance (ANOVA) followed by Dunnett's posthoc test. The following notations were used to describe statistical significance: $^{*}p<0.05$, $^{**}p<0.01$, $^{***}p<0.001$, $^{****}p<0.0001$, ns = not significant.

AUTHOR CONTRIBUTIONS

Fitz Gerald S. Silao: Conceptualization; data curation; formal analysis; visualization; writing – original draft; methodology; investigation; supervision; writing – review and editing; validation. **Valerie Diane Valeriano:** Data curation; formal analysis; visualization; writing – review and editing; investigation; methodology; validation. **Erika Uddström:** Data curation; investigation; visualization; methodology. **Emilie Falconer:** Data curation; methodology; investigation. **Per O. Ljungdahl:** Conceptualization; data curation; formal analysis; visualization; supervision; project administration; writing – review and editing; validation; funding acquisition; resources.

ACKNOWLEDGMENTS

The authors would like to thank the current and former members of the Per O. Ljungdahl, Claes Andréasson, and Sabrina Büttner laboratories (Stockholm University, Sweden) for their constructive comments throughout the course of this work. Gratitude is also extended to Kicki Ryman (Stockholm University, Sweden) and Sabrina Jenull (Medical University of Vienna, Austria) for fruitful discussions. We would also like to thank the following individuals for supplying strains: Valmik Vyas and Gerald R. Fink (MIT, USA), Karl Kuchler (Medical University of Vienna, Austria), Slavena Vylkova (Friedrich Schiller University, Germany), and Changbin Chen (Institute Pasteur of Shanghai, China). Lars Engstrand (Karolinska Institute, Sweden) is gratefully acknowledged for enabling the study of *Lactobacillus* co-culture in his laboratory and for the productive discussions. This research was supported by Swedish Research Council 2019-01547, 2022-01190 and Marie Curie—Initial Training Networks (ITN), ImResFun 606786 (POL).

CONFLICT OF INTEREST STATEMENT

Authors declare that they have no competing interests.

DATA AVAILABILITY STATEMENT

All data are available in the main text or the Supplementary Table S1.

ORCID

Fitz Gerald S. Silao https://orcid.org/0000-0002-4350-8395

REFERENCES

Alvarez, F.J., Ryman, K., Hooijmaijers, C., Bulone, V. & Ljungdahl, P.O. (2015) Diverse nitrogen sources in seminal fluid act in synergy to induce filamentous growth of *Candida albicans*. *Applied and Environmental Microbiology*, 81(8), 2770–2780. Available from: https://doi.org/10.1128/AEM.03595-14

Amorim-Vaz, S., Delarze, E., Ischer, F., Sanglard, D. & Coste, A.T. (2015) Examining the virulence of *Candida albicans* transcription factor mutants using Galleria mellonella and mouse infection models. *Frontiers in Microbiology*, 6, 367. Available from: https://doi.org/10.3389/fmicb.2015.00367

Antonenko, Y.N., Pohl, P. & Denisov, G.A. (1997) Permeation of ammonia across bilayer lipid membranes studied by ammonium ion selective microelectrodes. *Biophysical Journal*, 72(5), 2187–2195. Available from: https://doi.org/10.1016/S0006-3495(97)78862-3

Antonio, M.A., Hawes, S.E. & Hillier, S.L. (1999) The identification of vaginal Lactobacillus species and the demographic and microbiologic characteristics of women colonized by these species. *The Journal of Infectious Diseases.*, 180(6), 1950–1956. Available from: https://doi.org/10.1086/315109

Bottcher, B., Driesch, D., Kruger, T., Garbe, E., Gerwien, F., Kniemeyer, O. et al. (2022) Impaired amino acid uptake leads to global metabolic imbalance of *Candida albicans* biofilms. *NPJ Biofilms and Microbiomes*, 8(1), 78. Available from: https://doi.org/10.1038/s41522-022-00341-9

Brown, J.L., Delaney, C., Short, B., Butcher, M.C., McKloud, E., Williams, C. et al. (2020) Candida auris phenotypic heterogeneity determines pathogenicity in vitro. *mSphere*, 5(3), 1–15. Available from: https://doi.org/10.1128/mSphere.00371-20

Cueto-Rojas, H.F., Milne, N., van Helmond, W., Pieterse, M.M., van Maris, A.J.A., Daran, J.M. et al. (2017) Membrane potential independent transport of NH3 in the absence of ammonium permeases in Saccharomyces cerevisiae. *BMC Systems Biology*, 11(1), 49. Available from: https://doi.org/10.1186/s12918-016-0381-1

Danhof, H.A. & Lorenz, M.C. (2015) The *Candida albicans* ATO gene family promotes neutralization of the macrophage phagolysosome. *Infection and Immunity*, 83(11), 4416–4426. Available from: https://doi.org/10.1128/IAI.00984-15

Danhof, H.A., Vylkova, S., Vesely, E.M., Ford, A.E., Gonzalez-Garay, M. & Lorenz, M.C. (2016) Robust extracellular pH modulation by *Candida albicans* during growth in carboxylic acids. *mBio*, 7(6), 1–13. Available from: https://doi.org/10.1128/mBio.01646-16

de Boer, C.G. & Hughes, T.R. (2012) YeTFaSCo: a database of evaluated yeast transcription factor sequence specificities. *Nucleic Acids Research*, 40(Database issue), D169–D179. Available from: https://doi.org/10.1093/nar/gkr993

de Boer, M., Nielsen, P.S., Bebelman, J.P., Heerikhuizen, H., Andersen, H.A. & Planta, R.J. (2000) Stp1p, Stp2p and Abf1p are involved in regulation of expression of the amino acid transporter gene BAP3 of Saccharomyces cerevisiae. *Nucleic Acids Research*, 28(4), 974–981. Available from: https://doi.org/10.1093/nar/28.4.974

Eastment, M.C., Balkus, J.E., Richardson, B.A., Srinivasan, S., Kimani, J., Anzala, O. et al. (2021) Association between vaginal bacterial microbiota and vaginal yeast colonization. *The Journal of Infectious Diseases.*, 223(5), 914–923. Available from: https://doi.org/10.1093/infdis/jiaa459

Ehrstrom, S., Yu, A. & Rylander, E. (2006) Glucose in vaginal secretions before and after oral glucose tolerance testing in women with and without recurrent vulvovaginal candidiasis. *Obstetrics and*

Gynecology, 108(6), 1432–1437. Available from: https://doi.org/10.1097/01.AOG.0000246800.38892.fc

Erickson, R.J. (1985) An evaluation of mathematical models for the effects of pH and temperature on ammonia toxicity to aquatic organisms. *Water Research*, 19(8), 1047–1058.

Fernandes, T.R., Segorbe, D., Prusky, D. & Di Pietro, A. (2017) How alkalinization drives fungal pathogenicity. *PLoS Pathogens*, 13(11), e1006621. Available from: https://doi.org/10.1371/journal.ppat.1006621

Fisher, M.C. & Denning, D.W. (2023) The WHO fungal priority pathogens list as a game-changer. *Nature Reviews. Microbiology*, 21(4), 211–212. Available from: https://doi.org/10.1038/s41579-023-00861-x

Fukasawa, Y., Tsuji, J., Fu, S.C., Tomii, K., Horton, P. & Imai, K. (2015) MitoFates: improved prediction of mitochondrial targeting sequences and their cleavage sites. *Molecular & Cellular Proteomics*, 14(4), 1113–1126. Available from: https://doi.org/10.1074/mcp.M114.043083

Han, T.L., Cannon, R.D., Gallo, S.M. & Villas-Boas, S.G. (2019) A metabolomic study of the effect of *Candida albicans* glutamate dehydrogenase deletion on growth and morphogenesis. *npj Biofilms and Microbiomes*, 5, 13. Available from: https://doi.org/10.1038/s41522-019-0086-5

Hebert, E.M., Mamone, G., Picariello, G., Raya, R.R., Savoy, G., Ferranti, P. et al. (2008) Characterization of the pattern of alphas1- and beta-casein breakdown and release of a bioactive peptide by a cell envelope proteinase from *Lactobacillus delbrueckii* subsp. lactis CRL 581. *Applied and Environmental Microbiology*, 74(12), 3682–3689. Available from: https://doi.org/10.1128/AEM.00247-08

Hollomon, J.M., Liu, Z., Rusin, S.F., Jenkins, N.P., Smith, A.K., Koeppen, K. et al. (2022) The *Candida albicans* Cdk8-dependent phosphoproteome reveals repression of hyphal growth through a Flo8-dependent pathway. *PLoS Genetics*, 18(1), e1009622. Available from: https://doi.org/10.1371/journal.pgen.1009622

Huang, X., Chen, X., He, Y., Yu, X., Li, S., Gao, N. et al. (2017) Mitochondrial complex I bridges a connection between regulation of carbon flexibility and gastrointestinal commensalism in the human fungal pathogen *Candida albicans*. *PLoS Pathogens*, 13(6), e1006414. Available from: https://doi.org/10.1371/journal.ppat.1006414

Jang, S.J., Lee, K., Kwon, B., You, H.J. & Ko, G. (2019) Vaginal lactobacilli inhibit growth and hyphae formation of *Candida albicans*. *Scientific Reports*, 9(1), 8121. Available from: https://doi.org/10.1038/s41598-019-44579-4

Kammer, P., McNamara, S., Wolf, T., Conrad, T., Allert, S., Gerwien, F. et al. (2020) Survival strategies of pathogenic Candida species in human blood show independent and specific adaptations. *mBio*, 11(5), e02435-20. Available from: https://doi.org/10.1128/mBio.02435-20

Kasper, L., Seider, K., Gerwien, F., Allert, S., Brunke, S., Schwarzmuller, T. et al. (2014) Identification of Candida glabrata genes involved in pH modulation and modification of the phagosomal environment in macrophages. *PLoS One*, 9(5), e96015. Available from: https://doi.org/10.1371/journal.pone.0096015

Labotka, R.J., Lundberg, P. & Kuchel, P.W. (1995) Ammonia permeability of erythrocyte membrane studied by 14N and 15N saturation transfer NMR spectroscopy. *The American Journal of Physiology*, 268(3 Pt 1), C686–C699. Available from: https://doi.org/10.1152/ajpcell.1995.268.3.C686

Lagree, K., Woolford, C.A., Huang, M.Y., May, G., McManus, C.J., Solis, N.V. et al. (2020) Roles of *Candida albicans* Mig1 and Mig2 in glucose repression, pathogenicity traits, and SNF1 essentiality. *PLoS Genetics*, 16(1), e1008582. Available from: https://doi.org/10.1371/journal.pgen.1008582

Lin, Y.P., Chen, W.C., Cheng, C.M. & Shen, C.J. (2021) Vaginal pH value for clinical diagnosis and treatment of common vaginitis. *Diagnostics (Basel)*, 11(11), 1–12. Available from: https://doi.org/10.3390/diagnostics11111996

MacAlpine, J., Daniel-Ivad, M., Liu, Z., Yano, J., Revie, N.M., Todd, R.T. et al. (2021) A small molecule produced by Lactobacillus species blocks *Candida albicans* filamentation by inhibiting a DYRK1-family kinase. *Nature Communications*, 12(1), 6151. Available from: https://doi.org/10.1038/s41467-021-26390-w

Martinez, P. & Ljungdahl, P.O. (2005) Divergence of Stp1 and Stp2 transcription factors in *Candida albicans* places virulence factors required for proper nutrient acquisition under amino acid control. *Molecular and Cellular Biology*, 25(21), 9435–9446. Available from: https://doi.org/10.1128/MCB.25.21.9435-9446.2005

McCarthy, M.W. & Walsh, T.J. (2018) Amino acid metabolism and transport mechanisms as potential antifungal targets. *International Journal of Molecular Sciences*, 19(3), 1–12. Available from: https://doi.org/10.3390/ijms19030909

Miao, J., Willems, H.M.E. & Peters, B.M. (2021) Exogenous reproductive hormones nor *Candida albicans* colonization Alter the near neutral mouse vaginal pH. *Infection and Immunity*, 89(2), e00550-20. Available from: https://doi.org/10.1128/IAI.00550-20

Miller, E.A., Beasley, D.E., Dunn, R.R. & Archie, E.A. (2016) Lactobacilli dominance and vaginal pH: why is the human vaginal microbiome unique? *Frontiers in Microbiology*, 7, 1936. Available from: https://doi.org/10.3389/fmicb.2016.01936

Miramon, P. & Lorenz, M.C. (2016) The SPS amino acid sensor mediates nutrient acquisition and immune evasion in *Candida albicans*. *Cellular Microbiology*, 18(11), 1611–1624. Available from: https://doi.org/10.1111/cmi.12600

Miramon, P. & Lorenz, M.C. (2017) A feast for Candida: metabolic plasticity confers an edge for virulence. *PLoS Pathogens*, 13(2), e1006144. Available from: https://doi.org/10.1371/journal.ppat.1006144

Miramon, P., Pountain, A.W., van Hoof, A. & Lorenz, M.C. (2020) The paralogous transcription factors Stp1 and Stp2 of *Candida albicans* have distinct functions in nutrient acquisition and host interaction. *Infection and Immunity*, 88(5), 1–18. Available from: https://doi.org/10.1128/IAI.00763-19

Morales, D.K., Grahl, N., Okegbe, C., Dietrich, L.E., Jacobs, N.J. & Hogan, D.A. (2013) Control of *Candida albicans* metabolism and biofilm formation by Pseudomonas aeruginosa phenazines. *MBio*, 4(1), e00526-12. Available from: https://doi.org/10.1128/mBio.00526-12

Moyes, D.L., Wilson, D., Richardson, J.P., Mogavero, S., Tang, S.X., Wernecke, J. et al. (2016) Candidalysin is a fungal peptide toxin critical for mucosal infection. *Nature*, 532(7597), 64–68. Available from: https://doi.org/10.1038/nature17625

Navarathna, D.H., Harris, S.D., Roberts, D.D. & Nickerson, K.W. (2010) Evolutionary aspects of urea utilization by fungi. *FEMS Yeast Research*, 10(2), 209–213. Available from: https://doi.org/10.1111/j.1567-1364.2010.00602.x

Netea, M.G., Joosten, L.A., van der Meer, J.W., Kullberg, B.J. & van de Veerdonk, F.L. (2015) Immune defence against Candida fungal infections. *Nature Reviews. Immunology*, 15(10), 630–642. Available from: https://doi.org/10.1038/nri3897

Ng, K.Y.B., Mingels, R., Morgan, H., Macklon, N. & Cheong, Y. (2018) In vivo oxygen, temperature and pH dynamics in the female reproductive tract and their importance in human conception: a systematic review. *Human Reproduction Update*, 24(1), 15–34. Available from: https://doi.org/10.1093/humupd/dmx028

Ohsumi, Y., Kitamoto, K. & Anraku, Y. (1988) Changes induced in the permeability barrier of the yeast plasma membrane by cupric ion. *Journal of Bacteriology*, 170(6), 2676–2682.

Rane, H.S., Hayek, S.R., Frye, J.E., Abeyta, E.L., Bernardo, S.M., Parra, K.J. et al. (2019) *Candida albicans* Pma1p contributes to growth, pH homeostasis, and hyphal formation. *Frontiers in Microbiology*, 10, 1012. Available from: https://doi.org/10.3389/fmicb.2019.01012

Reuss, O., Vik, A., Kolter, R. & Morschhauser, J. (2004) The SAT1 flipper, an optimized tool for gene disruption in *Candida albicans*. *Gene*, 341, 119–127. Available from: https://doi.org/10.1016/j.gene.2004.06.021

Richardson, J.P., Ho, J. & Naglik, J.R. (2018) Candida-epithelial interactions. *Journal of Fungi (Basel)*, 4(1), 1–14. Available from: https://doi.org/10.3390/jof4010022

Richardson, J.P., Willems, H.M.E., Moyes, D.L., Shoaie, S., Barker, K.S., Tan, S.L. et al. (2018) Candidalysin drives epithelial signaling, neutrophil recruitment, and immunopathology at the vaginal mucosa. *Infection and Immunity*, 86(2), e00550-20. Available from: https://doi.org/10.1128/IAI.00645-17

She, X., Khamooshi, K., Gao, Y., Shen, Y., Lv, Y., Calderone, R. et al. (2015) Fungal-specific subunits of the *Candida albicans* mitochondrial complex I drive diverse cell functions including cell wall synthesis. *Cellular Microbiology*, 17(9), 1350–1364. Available from: https://doi.org/10.1111/cmi.12438

Silao, F.G.S., Jiang, T., Bereczky-Veress, B., Kuhbacher, A., Ryman, K., Uwamohoro, N. et al. (2023) Proline catabolism is a key factor facilitating *Candida albicans* pathogenicity. *PLoS Pathogens*, 19(11), e1011677. Available from: https://doi.org/10.1371/journal.ppat.1011677

Silao, F.G.S. & Ljungdahl, P.O. (2021) Amino acid sensing and assimilation by the fungal pathogen *Candida albicans* in the human host. *Pathogens*, 11(1), 5. Available from: https://doi.org/10.3390/pathogens11010005

Silao, F.G.S., Ryman, K., Jiang, T., Ward, M., Hansmann, N., Molenaar, C. et al. (2020) Glutamate dehydrogenase (Gdh2)-dependent alkalization is dispensable for escape from macrophages and virulence of *Candida albicans*. *PLoS Pathogens*, 16(9), e1008328. Available from: https://doi.org/10.1371/journal.ppat.1008328

Silao, F.G.S., Ward, M., Ryman, K., Wallstrom, A., Brindefalk, B., Udekwu, K. et al. (2019) Mitochondrial proline catabolism activates Ras1/cAMP/PKA-induced filamentation in *Candida albicans*. *PLoS Genetics*, 15(2), e1007976. Available from: https://doi.org/10.1371/journal.pgen.1007976

Smith, D.F.Q., Mudrak, N.J., Zamith-Miranda, D., Honorato, L., Nimrichter, L., Chrissian, C. et al. (2022) Melanization of *Candida auris* is associated with alteration of extracellular pH. *Journal of Fungi (Basel)*, 8(10), 1068. Available from: https://doi.org/10.3390/jof8101068

Sobel, J.D., Faro, S., Force, R.W., Foxman, B., Ledger, W.J., Nyirjesy, P.R. et al. (1998) Vulvovaginal candidiasis: epidemiologic, diagnostic, and therapeutic considerations. *American Journal of Obstetrics and Gynecology*, 178(2), 203–211. Available from: https://doi.org/10.1016/s0002-9378(98)80001-x

Subcommittee on Antifungal Susceptibility Testing (AFST) of the ESCMID. (2008) EUCAST definitive document EDef 7.1: method for the determination of broth dilution MICs of antifungal agents for fermentative yeasts. *Clinical Microbiology and Infection*, 14(4), 398–405. Available from: https://doi.org/10.1111/j.1469-0691.2007.01935.x

Swaminathan, K., Flynn, P., Reece, R.J. & Marmorstein, R. (1997) Crystal structure of a PUT3-DNA complex reveals a novel mechanism for DNA recognition by a protein containing a Zn2Cys6 binuclear cluster. *Nature Structural Biology*, 4(9), 751–759. Available from: https://doi.org/10.1038/nsb0997-751

Tebung, W.A., Omran, R.P., Fulton, D.L., Morschhauser, J. & Whiteway, M. (2017) Put3 positively regulates proline utilization in *Candida albicans*. *mSphere*, 2(6), 1–15. Available from: https://doi.org/10.1128/mSphere.00354-17

Teixeira, M.C., Viana, R., Palma, M., Oliveira, J., Galocha, M., Mota, M.N. et al. (2023) YEASTRACT+: a portal for the exploitation of global transcription regulation and metabolic model data in yeast biotechnology and pathogenesis. *Nucleic Acids Research*, 51(D1), D785–D791. Available from: https://doi.org/10.1093/nar/gkac1041

Todd, O.A., Noverr, M.C. & Peters, B.M. (2019) *Candida albicans* impacts Staphylococcus aureus alpha-toxin production via extracellular alkalinization. *mSphere*, 4(6), e00780-19. Available from: https://doi.org/10.1128/mSphere.00780-19

van de Wijgert, J.H., Borgdorff, H., Verhelst, R., Crucitti, T., Francis, S., Verstraelen, H. et al. (2014) The vaginal microbiota: what have we learned after a decade of molecular characterization? *PLoS One*, 9(8), e105998. Available from: https://doi.org/10.1371/journal.pone.0105998

Vazquez-Munoz, R. & Dongari-Bagtzoglou, A. (2021) Anticandidal activities by lactobacillus species: an update on mechanisms of action. *Frontiers in Oral Health*, 2, 689382. Available from: https://doi.org/10.3389/froh.2021.689382

Velasco, I., Tenreiro, S., Calderon, I.L. & Andre, B. (2004) Saccharomyces cerevisiae Aqr1 is an internal-membrane transporter involved in excretion of amino acids. *Eukaryotic Cell*, 3(6), 1492–1503. Available from: https://doi.org/10.1128/ec.3.6.1492-1503.2004

Vesely, E.M., Williams, R.B., Konopka, J.B. & Lorenz, M.C. (2017) N-acetylglucosamine metabolism promotes survival of *Candida albicans* in the phagosome. *mSphere*, 2(5), e00357-17. Available from: https://doi.org/10.1128/mSphere.00357-17

Vylkova, S. (2017) Environmental pH modulation by pathogenic fungi as a strategy to conquer the host. *PLoS Pathogens*, 13(2), e1006149. Available from: https://doi.org/10.1371/journal.ppat.1006149

Vylkova, S., Carman, A.J., Danhof, H.A., Collette, J.R., Zhou, H. & Lorenz, M.C. (2011) The fungal pathogen *Candida albicans* autoinduces hyphal morphogenesis by raising extracellular pH. *mBio*, 2(3), e00055-11. Available from: https://doi.org/10.1128/mBio.00055-11

Vylkova, S. & Lorenz, M.C. (2014) Modulation of phagosomal pH by *Candida albicans* promotes hyphal morphogenesis and requires Stp2p, a regulator of amino acid transport. *PLoS Pathogens*, 10(3), e1003995. Available from: https://doi.org/10.1371/journal.ppat.1003995

Wagner, G., Bohr, L., Wagner, P. & Petersen, L.N. (1984) Tampon-induced changes in vaginal oxygen and carbon dioxide tensions. *American Journal of Obstetrics and Gynecology*, 148(2), 147–150. Available from: https://doi.org/10.1016/s0002-9378(84)80165-9

Wagner, G. & Levin, R. (1978) Oxygen tension of the vaginal surface during sexual stimulation in the human. *Fertility and Sterility*, 30(1), 50–53. Available from: https://doi.org/10.1016/s0015-0282(16)43395-9

Wang, S., Wang, Q., Yang, E., Yan, L., Li, T. & Zhuang, H. (2017) Antimicrobial compounds produced by vaginal lactobacillus crispatus are able to strongly inhibit *Candida albicans* growth, hyphal formation and regulate virulence-related gene expressions. *Frontiers in Microbiology*, 8, 564. Available from: https://doi.org/10.3389/fmicb.2017.00564

Westman, J., Moran, G., Mogavero, S., Hube, B. & Grinstein, S. (2018) *Candida albicans* hyphal expansion causes Phagosomal membrane damage and luminal alkalinization. *mBio*, 9(5), e01226-18. Available from: https://doi.org/10.1128/mBio.01226-18

WHO. (2022) *WHO fungal priority pathogens list to guide research, development and public health action*. Geneva: World Health Organization.

Yang, T.H. & Wu, W.S. (2012) Identifying biologically interpretable transcription factor knockout targets by jointly analyzing the transcription factor knockout microarray and the ChIP-chip data. *BMC Systems Biology*, 6, 102. Available from: https://doi.org/10.1186/1752-0509-6-102

SUPPORTING INFORMATION

Additional supporting information can be found online in the Supporting Information section at the end of this article.

How to cite this article: Silao, F.G.S., Valeriano, V.D., Uddström, E., Falconer, E. & Ljungdahl, P.O. (2024) Diverse mechanisms control amino acid-dependent environmental alkalization by *Candida albicans*. *Molecular Microbiology*, 121, 696–716. Available from: https://doi.org/10.1111/mmi.15216